Recent advances of high entropy alloys for aerospace applications: a review

Modupeola Dada
Department of Chemical, Metallurgical and Materials Engineering, Tshwane University of Technology, Pretoria, South Africa
Patricia Popoola
Tshwane University of Technology, Pretoria, South Africa, and
Ntombi Mathe
Council for Scientific and Industrial Research, Pretoria, South Africa

Abstract

Purpose – This study aims to review the recent advancements in high entropy alloys (HEAs) called high entropy materials, including high entropy superalloys which are current potential alternatives to nickel superalloys for gas turbine applications. Understandings of the laser surface modification techniques of the HEA are discussed whilst future recommendations and remedies to manufacturing challenges via laser are outlined.

Design/methodology/approach – Materials used for high-pressure gas turbine engine applications must be able to withstand severe environmentally induced degradation, mechanical, thermal loads and general extreme conditions caused by hot corrosive gases, high-temperature oxidation and stress. Over the years, Nickel-based superalloys with elevated temperature rupture and creep resistance, excellent lifetime expectancy and solution strengthening L12 and $\gamma^{¨}$ precipitate used for turbine engine applications. However, the superalloy's density, low creep strength, poor thermal conductivity, difficulty in machining and low fatigue resistance demands the innovation of new advanced materials.

Findings – HEAs is one of the most frequently investigated advanced materials, attributed to their configurational complexity and properties reported to exceed conventional materials. Thus, owing to their characteristic feature of the high entropy effect, several other materials have emerged to become potential solutions for several functional and structural applications in the aerospace industry. In a previous study, research contributions show that defects are associated with conventional manufacturing processes of HEAs; therefore, this study investigates new advances in the laser-based manufacturing and surface modification techniques of HEA.

Research limitations/implications – The AlxCoCrCuFeNi HEA system, particularly the Al0.5CoCrCuFeNi HEA has been extensively studied, attributed to its mechanical and physical properties exceeding that of pure metals for aerospace turbine engine applications and the advances in the fabrication and surface modification processes of the alloy was outlined to show the latest developments focusing only on laser-based manufacturing processing due to its many advantages.

Originality/value – It is evident that high entropy materials are a potential innovative alternative to conventional superalloys for turbine engine applications via laser additive manufacturing.

Keywords Aerospace applications, High entropy alloys, High entropy materials, Laser surface modification

Paper type Literature review

1. Introduction

Throughout the years, alloys used commercially are structured by choosing an element as a base with the addition of essential solutes to improve the properties of the base component (Chatterjee *et al.*, 2009; Gao and Alman, 2013). The elemental composition of these combinations was reduced to avoid the development of mass intermetallic mixes existing within the molar atomic proportions of these alloys, hence, attaining 40% atomic percentages or more. These intermetallic phases reduce the quality of the alloys whilst in service (Chen *et al.*, 2018c; Hummel, 2004); The possibilities of fabricating alloys with an atomic percentage between 5 and 35 in a composition comprising at least five principal elements were further investigated (Cantor *et al.*, 2004).

According to Ye *et al.* (2016), a new class of alloys was discovered with enhanced attributes compared with conventional alloys by mixing several principal elements in equimolar or near equimolar variations. Yeh *et al.* (2004) named the alloys "High Entropy Alloys" (HEAs). The authors defined HEAs as amalgams having compositions with at least five principal metallic elements and having a molar atomic

The current issue and full text archive of this journal is available on Emerald Insight at: **https://www.emerald.com/insight/1708-5284.htm**

World Journal of Engineering
20/1 (2023) 43–74
 [ISSN 1708-5284]
[DOI 10.1108/WJE-01-2021-0040]

The authors will like to appreciate Prof. Sisa Pityana at the Council for Scientific and Research (CSIR), the National Laser Center (Laser Enabled Manufacturing Resource Group), Prof. Samson Adeosun from the Department of Metallurgical and Materials Engineering, University of Lagos, Mr Juwon Ojo Fayomi and Uyor Uwa Orji at the Surface Engineering Research Laboratory (SERL), Tshwane University of Technology, Pretoria, South Africa for their technical support during this research.

Received 21 January 2021
Revised 23 May 2021
Accepted 17 June 2021

proportion between 5% and 35% (Joseph, 2016). Studies on HEAs have concluded that most HEAs comprise simple face centered cubic (FCC), body-centered-cubic (BCC) or Hexagonal-Closed-Packed solid solutions phase attributed to their thigh-entropy effect (Kuehl and Kuehl, 2000). Wang *et al.* (2009) reported that the characteristic features of solid solution phases give HEAs outstanding properties such as strength, extraordinary mechanical and physical properties at cryogenic temperatures, plastic strain, fracture strength and good ductility; they possess elevated-temperature oxidation resistance and excellent work hardenability and have been reported to possess distinctive magnetic and tribological properties (Gludovatz *et al.*, 2014; Mishra and Shahi, 2018).

Furthermore, Senkov *et al.* (2010) reported HEAs as exceptional refractory materials and their fatigue resistance exceeding conventional alloy, according to Hemphill (2012). They possess surface layers that are resistant to corrosion and they have diffusion barrier layers for various structural applications (Qiu *et al.*, 2017). Nonetheless, the study of the thermodynamics of HEAs is the study of energy transformation from one form to another, where the difference between the reactant and the product is favourable. Brown *et al.* (2005) stated that chemical thermodynamics can predict if a reaction is spontaneous or not (Olumayegun *et al.*, 2017). Tancret *et al.* (2017) reported using thermodynamics in designing new HEA compositions by observing the laws. The first law states that work and heat are forms of energy that can be transformed but cannot be created or destroyed (Atkins, 2010). The second law emphasizes that entropy is the degree of any disorder in any system, including the HEA system and the level of disorder in an isolated system increases in spontaneous processes (Brandao *et al.*, 2015). As a result, the second law predicts that the degree of disorderliness of a system will increase with time because matter always tends towards chaos. The third law states that the degree of disorderliness of a crystal reaches zero as the temperature of the system also approaches zero (Bera *et al.*, 2016; Masanes and Oppenheim, 2017).

Consequently, the energy transformation of HEAs' system in constant temperature called isothermal conditions will be at equilibrium when the free energy (G) of that system is at the barest minimum and $G = H - TS$, where H denotes the Enthalpy of formation, T is the Temperature, S is the Entropy and then G symbolizes the Gibbs free energy. G is defined as the thermodynamic capability of the HEAs, which calculates the maximum work performed by the thermodynamic structure at isothermal environments and pressure. Enthalpy is the total heat contained in the HEAs system and it is the core energy of the system in addition to the product of the volume and pressure (Otto *et al.*, 2013). Whilst Entropy can be defined as the extent of randomness in HEAs system, it is the unavailability of the system's thermal energy to convert into mechanical work (Rusanov, 2016).

HEAs are at equilibrium attributed to their high entropy effect that minimizes the Gibbs free energy because of an increased amount of elements in its composition. Therefore, $\Delta G_{mix} = \Delta H_{mix} - T\Delta S_{mix}$ and according to Boltzmann's hypothesis, $\Delta S_{mix} = RIn_{(n)}$, where ΔS_{mix} is the mixing entropy, R denotes the gas constant and (n) defined as the total number of elements in the mixture (Miracle, 2017).

Compositions with one or two elements have $\Delta S_{conf} < 1\,R$. Composition with two to four elements have $\Delta S_{conf} < 1.5\,R$ whilst HEAs with compositions of five or more elements have $\Delta S_{conf} < 1.5\,R$ as shown in Figure 1. ΔS_{mix} has four contributors; electronic randomness, vibration, magnetic dipole and configuration entropy; configuration entropy is central to all contributors (IkedaGrabowski and Körmann, 2019). The configuration entropy increases when the amount of elements in the HEA system increases. According to Jien-Wei (2006), there should be at least five elements and a maximum of 13 elements in the HEA system to make the high mixing entropy good enough to counter the mixing enthalpy and reduce the Gibbs free energy to its barest minimum causing entropic stabilization of a disordered solid solution system with fine microstructures (Otto *et al.*, 2013).

A composition above 13 elements suggests that there will be little or no benefit to the system by adding a greater number of elements to the HEA system, however, the concentration of each element must be between 5% and 35% (GorsseCouzinié and Miracle, 2018). For example, the AlCoCrCuFeNi compositional design has six elements with the configurational entropy of 1.79 R and atomic concentrations between 5%–35% making the HEA's system thermodynamically favourable according to Boltzmann's theory. This compositional theory has its pros and cons. Zhang and Zhou (2007) proposed that the criterion for alloy design must have the mixing enthalpy of the system between $(-40) \sim (+10)$ KJ/mol and that the maximum radius difference should be less than 12%. The authors were more convinced that the design conditions were majorly on the mixing entropies based on Boltzmann's theory with a minimum of 1.36 R and the enthalpy of mixing of the system should be very close to zero with a minimum of the atomic size difference of 4.6 between the elements in the composition.

Zhang *et al.* (2012a) predicted that only two parameters are important for phase formation; δ and Ω, where Ω is defined as the product of the mixing enthalpy, the entropy of mixing of the HEA system and the melting temperature. Whilst δ of the system is the average variance of the element's atomic radius. Accordingly, if a combination of $15 \leq \Delta H_{mix}^{liq} \leq +5$ kJ/mol and $\leq 5\%$ is met, the solid solution disordered phase is favoured. King *et al.* (2016) also mentioned that the ϕ value

Figure 1 Compositional mixing entropies (Ye *et al.*, 2016)

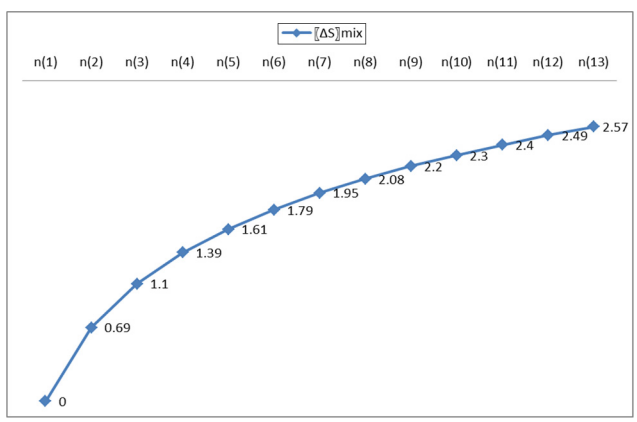

gives an estimate to single-phase HEAs formation and stability, where ϕ is defined as the percentage between the G of a disordered solid solution and the segregated binary system. A total of 73 elements were gotten from the periodic table to satisfy the $\phi \geq 1$ and $\delta \leq 6.6$ in the scale of their properties. About 186,299,362 equimolar systems were screened in the process (1,088,431 with 4-elements composition, 15,020,335 with 5-elements composition and 170,230,452 with 6-element composition). In 1970 single-phase HEAs were recognized (636 with 4-element composition, 983 with 5-element composition and 306 with 6-element composition). The authors established that the parameters $\Omega \geq 1.1$ and $\delta \leq 6.6\%$ favour the growth of a stable solid solution, yet, these observations were all based on experimental data which may not always be true because the authors did not take into account the competing phases in the system (Gao and Alman, 2013).

According to Song *et al.* (2017), another criterion for designing HEAs is through energy-dispersive x-ray spectroscopy; this technique used alongside transmission electron microscopy (TEM) may be able to detect x-rays emitted from the alloys when the alloy is attacked by an electron beam which can then be analysed. At the point of attack, the element's atomic-scale modulation creates fluctuation of different lattice resistance. This lattice resistance shows the dislocation behaviour of the alloy and provides in-depth knowledge of the HEA's properties (Ding *et al.*, 2019).

In a review by Chen *et al.* (2018c), the fundamentals of multi-principal elemental mixtures of HEAs result in four core effects; Sluggish diffusion attributes to the growth of amorphous structures or monocrystalline structures. The Lattice Distortion dictates the properties of the alloy whilst the high entropy effect contributes to the merging of alloys having compatible elements and composed of solid solution phases or one single phase. The cocktail effect relies on the property contribution of each principal element in the composition (Miracle, 2017; Yeh, 2013). Despite the improvement of the advanced material properties attributed to these core effects, some reports state that the solid solution strengthening of HEAs is low at elevated temperatures. He *et al.* (2016) tried precipitation hardening of HEAs using $L2_1$ precipitates to improve its strength whilst Gwalani (2017) used B2 precipitates to develop hardenable HEAs. There were improvements in the mechanical properties at room temperatures; nonetheless, at temperatures above 500°C, the strength of the alloy decreases limiting its applications until recently (LiuYang and Liu, 2018).

The high-temperature characteristics of materials used for turbine engine applications reduce fuel consumption, operating costs and pollution. These superalloys are used in the aerospace industry because of their strength, resistance to degradation in oxidizing environments, toughness and density as required properties during service in harsh conditions at elevated temperatures. Nickel-based, iron-based, titanium-based and cobalt-based superalloys are typical alloys with these attributes; however, most of these superalloys are not stable at elevated temperatures. Superalloys having a maximum service temperature of 649°C at room temperature also have a negative lattice misfit, poor thermal conductivity and are difficult to machine. Therefore, in this study, the advances of HEAs as a new class of material with potential applications in the aerospace industry as a potential replacement for Nickel super alloys, aluminum, steel, magnesium and titanium alloys are proposed. Gas turbine engines are combustion devices that use air as its working fluid to extract the chemical energy from fuel, transforming it into mechanical energy to drive the propeller and engine of an aeroplane (Walsh and Fletcher, 2005).

The energy created is usually low and backed up with step-up transformers to increase the voltage capacity. In the aerospace industry, turbo compressors and generators are the most common applications for gas turbines. The turbine engine consists of a theoretical cycle which is a reversible procedure and characterized by extended life spans, minimal moving parts and maintenance, therefore, managing the combustion to produce the required amount of pressure into the exhaust gas is vital (Viteri and Anderson, 2003). The turbine engine is designed to dictate its performance requirements determined by the shaft powerhouse in certain extreme temperature conditions, therefore, high-performance materials with new advances are necessary to withstand these conditions (Li and Nilkitsaranont, 2009). The components of a turbine engine are selected due to their lightweight which helps conserve fuel and their weight or thrust ratio. The Nickel superalloy as a turbine engine material is mostly used for disks, blades, combustion liners, burners, vanes and thermal barrier coatings. The superalloy is composed of Nickel as the based element with additions of Al, Ti, Co, B, Mo, W and N alongside other elements to improve the properties of the superalloy. Nickel superalloy has good ductility, thermal stability and resistance to corrosion and creep attributed to their precipitate microstructure and grain size.

Ding *et al.* (2018) stated that rhenium segregates by dislocation pipe diffusion to form a Cottrell atmosphere and this enhances the creep resistance of Nickel-based superalloys. However, according to QianDing and Zhu (2018), nickel-based superalloy is hard to machine when used for aero-engine applications and the working temperature of Inconel 718 and 800 superalloy no longer meets the high temperature of the combustor and high pressure of the turbine (Gupta *et al.*, 2019). Wang *et al.* (2019b) reported that nickel-based superalloys fabricated via powder metallurgy are prone to abnormally large grains especially during super Solvus heat treatments and the mechanism behind this growth which is harmful to the superalloy in-service performance is not fully understood whilst Lin *et al.* (2017) stated that the hot deformation characteristics of the superalloy are complicated whilst Waspaloy with wide application for gas turbine disks has been reported to be subjected to elevated temperature creep deformation (Birosca *et al.*, 2019).

GH2 132 is a high-temperature iron-based superalloy with age-hardening characteristics suitable for turbine blades, casings, fasteners and wheels (De Cicco *et al.*, 2004). It has fine particles with a strengthening γ'' phase when heat treated, giving the superalloy good plasticity and strength. According to AntonialliCarvalho and Diniz (2020), iron-based superalloys cost lower than other superalloys, however, the superalloy lacks most properties that other superalloys possess. Tian *et al.* (2017) reported that the superalloy has poor thermal stability, elevated temperature strength and very hard to machine (Tan *et al.*, 2008). On the other hand, cobalt-based superalloy with

Table 1 Properties of materials used for turbine engine applications

Material	Density (g/cm3)	Yield strength (MPa)	Hardness (HV)	Thermal stability	Phase structure	Benefits	Limitations	Ref
HESA	7.78–7.94	500	300–350	Excellent	$L1_2$, γ'' nanosized precipitate	Good compressive strength, high temperature ultimate tensile strength, lightweight and creep resistant	Still under investigation	(TsaoYeh and Murakami, 2017), (Yeh and Tsao, 2019),(Whitfield *et al.*, 2020), (Dada *et al.*, 2021)
Iron-based super alloy	7.94	275	280	Good	γ and γ''	Room-temperature strength, high-temperature strength, creep, wear and oxidation resistance	Difficult to machine, poor service performance, susceptible to defects, hot corrosion degradation	(Chawla *et al.*, 2009; Moody *et al.*, 2001; Sidhu *et al.*, 2007),(Cabibbo *et al.*, 2008)
Nickel-based super alloy	7.8–9.4	275	370	Good	FCC, γ'', FCC carbides, ordered orthorhombic intermetallic phases and body-centred tetragonal γ'''	High Solvus and melting temperature, solid-solution strengthening and creep resistance	Instability at high temperatures, difficult to machine and low thermal conductivity	(Wang *et al.*, 2017), (Ogunbiyi *et al.*, 2019a), (Ogunbiyi *et al.*, 2019b), (Vilaro *et al.*, 2012)
Cobalt-based super alloy	>9.0	621	407	Good	$\gamma + \gamma''$, $L1_2$ ordered precipitates and TCP	High operating temperature, thermal shock, creep and corrosion resistance	Low strength compared to other superalloys	(Chung *et al.*, 2020a; MakineniNithin and Chattopadhyay, 2015), (TiradoTaylor and Dunand, 2019), (Zhang *et al.*, 2013)
Titanium-based super alloy	4.41	1,561	346	Good	γ, FCC $L1_2$	High strength- toughness and fatigue strength, corrosion-resistant	Low adhesive, high friction coefficient, low ductility	(Clemens and Smarsly, 2011; Peters *et al.*, 2003), (Long *et al.*, 2013),(Yan *et al.*, 2016), (Farotade and Popoola, 2017)

γ/γ'' structure has good wear resistance, oxidation and melting temperatures higher than the nickel-based superalloy. Chung *et al.* (2020b) reported that the addition of chromium to cobalt-based superalloys improves the oxidation resistance but adversely affects the creep performance. The superalloy has poor creep resistance, limiting the superalloy's usage in high-stress applications (Jokisaari *et al.*, 2017). Bocchini *et al.* (2017) suggested microalloying the superalloy with Boron to improve the creep strength. Conversely, studies showed that precipitating borides formed decreased the yield strength of superalloys (KrolBaither and Nembach, 2004). Titanium superalloy used for aerospace applications, also known as Ti6Al4V, is a low density, high strength and fracture toughness, biocompatible material with excellent corrosion resistance (Boyer, 1996). These attributes make the alloy suitable for aircraft structural applications, yet the alloy has poor thermal conductivity and tribo-behaviour (PhilipMathew and Kuriachen, 2019).

Nickel, iron and cobalt-based superalloys are used as parts of an engine and they are usually components for the turbine and combustor compartments due to their lightweight to reduce fuel consumption. However, nickel-based superalloys are prone to accelerated corrosion and oxidation triggered by Sulphur in the fuel used to power these engines. Therefore, cobalt-based superalloys are preferred as replacements. Furthermore, the iron-based superalloy used for the compressor and fan of the turbine engine undergoes temperatures at 600°C, making titanium alloys the preferred alternative for this application. Thus, an increasing need for elevated-temperature, high-efficiency material with improved properties, coupled with the substantial limitations of conventional superalloys, makes the advances of HEA material a potential alternative to replace conventional superalloys for aerospace applications.

2. Advances in material technology: high entropy materials

The innovation of HEAs has spread to other facets of material developments including, ceramics, steel, polymers, films and superalloys. The characteristic high entropy mixing effect enhances the formation of solid solution phases at elevated temperatures leading to refined microstructures and properties for applications in the aerospace industry, thus becoming an emerging field of research for many researchers (Yeh and Lin, 2018). Opportunities in this field of study include but are not limited to the development of low, medium-entropy and high-entropy alloys with more principal elements in the composition in comparison with conventional materials consisting of only one or two elements. The activation of the whole periodic table in material design and development forms single solid solution or amorphous phases and the fabrication of these materials having improved properties at room and elevated temperatures with diverse applications in several industries (Zhang, 2019). In recent times, there have been different designs of the HEA concept, such as refractory HEAs (RHEAs) are alloys consisting of five or more refractory principal elements whilst refractory complex concentrated alloys containing three or more major elements in design (Senkov *et al.*, 2018b). Senkov *et al.* (2010) fabricated the first two near-equiatomic RHEAs consisting of W-Nb-Mo-Ta and V via arc melting. The alloys had BCC solid solution structures with low densities and high hardness attributed to the solid solution strengthening mechanism. This discovery brought immediate attention to the alloy's characteristic attribute to retain its strength at elevated temperatures (Gao *et al.*, 2015). A broad investigation of other refractory materials consisting of Ti, Hf, Zr and Cr has as been reported with additions of non-refractory elements such as Ni, Si, Al and Co (Juan *et al.*, 2015; Lilensten *et al.*, 2014; SenkovSenkova and Woodward, 2014).

Interstitial HEAs (iHEAs) were developed to improve the mechanical properties of HEAs by the addition of interstitial elements such as carbon, hydrogen, nitrogen and boron (Baker, 2020; Lu *et al.*, 2019a; Seol *et al.*, 2020; Ye *et al.*, 2020). The influence of interstitial elements on HEAs depends on the content, compositional homogeneity and microstructure of the HEAs (Li, 2019). Chen *et al.* (2018b) studied the influence of carbon on the properties of as-cast CoCrFeMnNi HEA and the results showed that the minor addition of the interstitial element improved the mechanical properties of the alloy, however; very high carbon content reduced the ductility of the alloy. Suggesting that only a minor addition is required for the property enhancement of the HEA as interstitial elements have been reported to be effective in improving the strength of HEAs attributed to their ability to influence the interaction of dislocations causing higher lattice distortions, changing the stacking fault energy and phase stability of the iHEAs (Saeed-Akbari *et al.*, 2009; WuParish and Bei, 2015). Li and Raabe (2018) investigated the effect of compositional inhomogeneity on the properties of dual-phase non-equiatomic $Fe_{49.5}Mn_{30}Co_{10}Cr_{10}C_{0.5}$ iHEAs prepared via cold-rolling, recrystallization annealing and hot rolling. Results showed that the strain-hardening ability and ductility of the iHEA reduced attributed to the compositional inhomogeneity (Chang *et al.*, 2019; Guo *et al.*, 2019).

HEAs prepared by mechanical alloying (MA) sometimes result in nanocrystalline structures which possess thermal, mechanical and magnetic properties for aerospace, biomaterials and energy applications and these HEAs with nanoparticles are called nanocrystalline HEAs (HEA-NPs) (Koch, 2017; Zou *et al.*, 2017). VaralakshmiKamaraj and Murty (2008) fabricated the Al-FE-Ti-Cr-Zn-Cu HEA-NPs system via MA and the results showed that the HEA-NPs had a BCC structure with crystal sizes of less than 10 nm remaining stable after heat treatments at 800°C for 1 h having a density of 99%. There are also reports of HEA- NPs forming multiple phases after MA (Fu *et al.*, 2013). However, MA is plagued with several challenges such as contaminations, time consumption due to large milling times and phase transformations. Therefore, KumarTiwary and Biswas (2018) investigated another approach to attaining HEA-NPs asides from MA by first fabricating the alloys using arc melting casting then crushing the ingot via cryomilling. The authors selected $Cu_{0.2}Ag_{0.2}Au_{0.2}Pt_{0.2}Pd_{0.2}$, $Fe_{0.2}Cr_{0.2}Mn_{0.2}Ni_{0.2}Co_{0.2}$ and $Fe_{0.2}Cr_{0.2}Mn_{0.2}V_{0.2}Al_{0.2}$ HEAs because these alloys exhibit FCC phases which are relatively difficult to crush attributed to their ductility. The results showed that 10 nm-sized HEA-NPs were formed after cryomilling at 123 K for a few hours without phase transformations or contaminations after cyromilling (Liu *et al.*, 2012).

In the past decade, researchers designed and fabricated several HEAs based on selecting multi principal elements through equiatomic or near equiatomic substitutions. The $Al_xCoCrCuFeNi$ system, where x denotes the molar ratio, has the $Al_{0.5}CoCrCuFeNi$ HEA, in particular, widely studied for its outstanding properties and known to surpass steels and titanium alloys. The alloy system exhibits structural stability at elevated temperatures, excellent ductility, strain hardening ability and mechanical properties which make the alloy a potential material component for applications in extreme environments (Microstructure and mechanical properties of the brazed region in the AlCoCrFeNi high-entropy alloy and FGH98 superalloy joint). In 2005, Tong *et al.* (2005) considered the mechanical properties of the AlxCoCrCuFeNi system via the arc melting and casting method. The authors stated that the alloys exhibited promising mechanical properties with excellent elevated temperature strength and wear resistance. The alloys showed a strong BCC phase to ductile FCC phase strengthened by the solid solution of the aluminium atoms varied from 0 to 5.0.

In the same year, Chen *et al.* (2005) studied the $Al_{0.5}CoCrCuFeNi$, $Al_2CoCrCuFeNi$ and AlCrNiSiTi alloy system using a reactive sputtering technique with nanostructures nitride and metallic films. The alloys showed simple BCC and FCC solid crystal solutions. However, they observed that the crystallinity of the alloy decreased with an increase in the nitrogen flowrate in the chamber where the alloys reached an amorphous structure. The TEM, Field Emission Scanning Electron Microscopy and Atomic Force Microscope observations showed that the morphology and structure evolution of the film was different between AlxCoCrCuFeNi and AlCrNiSiTi HEAs. The slope of films resistivity was much steeper in AlCrNiSiTi than in AlxCoCrCuFeNi HEA. The hardness enhancement by nitrides was inferior in AlCrNiSiTi than in AlxCoCrCuFeNi HEAs.

The following year, Wu *et al.* (2006) explored the AlxCoCrCuFeNi alloy's adhesive wear behaviour at different aluminium content via arc melting. The authors noticed that the BCC phase volume fraction and microhardness increased as the wear coefficient decreases with the mechanism changing from delamination o oxidation wear. At a lower aluminium content of x = 0.5, the alloy was a simple ductile FCC phase which was deeply grooved due to periodic delamination resulting in large debris, however, at x = 1.0 the alloy exhibited an FCC and BCC phase showing that an increase in the aluminium content promotes the BCC phase. The surface was worn and deeply grooved but only at the FCC region with dominant delamination wear whilst the BCC region showed oxidative wear with high oxygen content but with no grooves on the smooth surface. The authors attributed the improvement in wear resistance to the excellent hardness properties.

Chen *et al.* (2006) scrutinized the influence of vanadium on the microstructure of arc melted $Al_{0.5}CoCrCuFeNi$ HEA. The results showed that the alloy consisted of an FCC phase with little vanadium content but as the vanadium content increases to 0.4, the BCC structure was observed with spinodal decomposition enveloping the FCC dendrites and a peak in the microhardness values were observed. This shows that increasing the vanadium content also promotes the BCC solid solution phase and the hardness of the alloy. The wear resistance of the alloy was investigated, and there was also an increase in the wear resistance with an increase in the vanadium content. The authors concluded by stating that the optimal vanadium content addition to the $Al_{0.5}CoCrCuFeNi$ system is between x = 1.0 and 1.2.

In 2008, Li *et al.* (2008) added other elements to the AlxCoCrCuFeNi alloy system in equal molar ratios via arc melting. The effects of Mn, Ti and V were studied and the results indicated that the addition of Mn showed a similar microstructure with the parent AlCoCrCuFeNi alloy except for the long strips of chromium-rich phases observed. However, the addition of Ti completely changed the structure from dendritic to eutectic cells. These authors also confirmed that the vanadium addition gave the best ductility and strengthening effect. Chen and Wong (2008) studied the AlxCoCrCuFeNi composition using magnetron sputtering using homogenous alloy targets. The authors revealed that the alloy had a cubic spinel phase without any oxide phases and increased microhardness values. They observed a loss in the film's conductivity but an increase in the optical transmittance with an increase in aluminium content. The decrease in conductivity is attributed to the reduction in available carriers with an increase in aluminium content, which affects the number of conducting cations available at the octahedral sites. The Hall measurements revealed a p-type conducting behaviour for the $Al_{0.5}CoCrCuFeNi$ oxide film with a conductivity of 40.1 $\Omega^{-1}cm^{-1}$, a carrier density of $5.81 \times 1{,}018\,cm^{-3}$ and mobility as high as 43.2 $cm^2V^{-1}s{-}^{1}$. Moreover, Hall measurements show metallic conduction behaviour for the $Al_{0.5}CoCrCuFeNi$ oxide film and thermally activated semiconducting properties for the $Al_1CoCrCuFeNi$ and $Al_2CoCrCuFeNi$ oxide films.

The deformation behaviour of arc melted $Al_{0.5}CoCrCuFeNi$ alloy was studied by Tsai *et al.* (2009). The study revealed that the alloy had excellent workability and exhibited a large work hardening capacity in both hot forging and cold rolling. The main deformation and hardening mechanisms during cold work are uniquely associated with the Nano twinning deformation of this alloy. The easy formation of Nano twins appears to result from the blockage by the Widmanstätten Cu-rich precipitates of local slip deformation in a space of several tensile of nanometers, and the low stacking fault energy, which promotes the nucleation of Nano twins. This alloy was fully annealed in 5 h at 900°C, revealing significantly higher resistances to static anneal softening than traditional alloys with comparable melting points. This resistance is attributable to extensive solution hardening, low stacking fault energy and the effect of sluggish diffusion on HEA.

Tang and Yeh (2009) inspected the vacuum arc melted $Al_xCoCrCuFeNi$ (HEAs) developed for wear-resistant structural parts with plasma nitride at 525°C for 45 h and using different aluminium contents (x = 0 to 1.8). They mentioned that the nitride layer is composed of CrN, Fe_4N and AlN which comprises an un-nitrided copper-rich interdendrite phase and a nitride dendrite phase. The authors noticed an increased amount of FCC phase in AlN was as a result of the larger consumption of aluminium whilst the increased amount of BCC phase in CrN and Fe_4N after nitriding was due to the increased Al content of the substrate caused by the larger consumption of chromium and iron. The alloy system provides

a wide range of substrate hardness from 170 HV to 560 HV before nitriding, which becomes harder after nitriding. The results showed that the nitride samples had superior wear resistance, layer thickness and substrate hardness than the un-nitrided samples.

Ng *et al.* (2012) on the stability of solid solution phases in HEAs reported in the literature were inconclusive, thus the authors used a series of thermo-mechanical treatments to study the stability of the solid solution phases in a vacuum arc melted $Al_{0.5}CoCrCuFeNi$ HEA. Intermetallics and solid solution phases were observed, however, the authors observed that the solid solution phases were stable against the intermetallic compounds, high temperatures $> 850°C$ and at low temperatures $< 300°C$. At intermediate temperatures, however, the intermetallic δ-phase co-existed with the solid solution phases. The authors mentioned that the mechanism for the phase stability was reported to be influenced by the core effects; the high entropy effect between the solid solution phases and intermetallic compounds in $Al_{0.5}CoCrCuFeNi$ alloy and the sluggish diffusion kinetics accounted for the equivalent quenched-in of the phases from elevated temperature to room temperature and the high entropy effect also accounted for a simple phase of mainly two FCC structures.

Hemphill *et al.* (2012) scrutinized the fatigue behaviour of arc melted $Al_{0.5}CoCrCuFeNi$ HEA. The results showed that alloy had good fatigue resistance due to prolonged fatigue lives at relatively high stresses compared with steels and titanium alloys. However, microstructural defects such as aluminium oxide and micro cracks were observed, and this was attributed to the manufacturing process. The authors concluded that the reduction of the defects will cause improved fatigue resistance, exceeding conventional alloys. In 2015, Tang *et al.* (2015b) also probed the fatigue behaviour of cold-rolled $Al_{0.5}CoCrCuFeNi$ HEA. Some samples were fabricated using high-purity components whilst others were fabricated with commercial-purity components. The results of the scatter plot showed that the high-purity samples had less scatter, but the fatigue behaviour of the alloy was comparable to commercial alloys. The authors also observed nano-twinning behaviour which resulted in the strengthening of the alloy, nonetheless; the authors suggested that using advanced manufacturing techniques in fabricating the alloy may enhance the fatigue behaviour of the alloy. $Al_{0.5}CoCrCuFeNi$ HEA is inevitably subjected to some amount of drying induced shrinkage during manufacture. When shrinkage is restrained, either internally or externally, tensile stresses develop and potentially cause micro-cracking. Research has shown that drying-induced micro-cracks which act as crack initiation sites usually at the surface will facilitate the transport of aggressive agents and this will reduce the fatigue life of the material.

From the literature reviewed, the $Al_xCoCrCuFeNi$ HEA system, particularly the $Al_{0.5}CoCrCuFeNi$ HEA possesses good mechanical and physical properties exceeding that of pure metals. Fisher (2015, p. 28) recounted that the $Al_{0.5}CoCrCuFeNi$ HEA possesses good thermal stability. With an increase in heat treatment temperature; the phase structure and hardness of the alloy were stable. The authors reviewed the effect of heat treatment on the microstructure and hardness of $Al_{0.5}CoCrCuFeNi$ HEAs prepared in water-cooled copper crucible vacuum induction levitation melting. The microstructure and phase structure of the alloy remained stable by the different cooling methods, but the hardness of the alloy after furnace cooling was higher than those air-cooled and water-cooled. Tabachnikova *et al.* (2017), summarized the mechanical and fracture characteristics of the high-entropy alloy $Al_{0.5}CoCrCuFeNi$ in the temperature range 0.5–300 K for different structural states (as-cast and after two heat treatments).

The temperature dependences of Young's modulus for different structural states were measured by mechanical resonance spectroscopy and an increase in the Young's modulus was recorded. Its outstanding strength is comparable to some metallic glasses and that of structural ceramics. The $Al_{0.5}CoCrCuFeNi$ HEA has been reported to be a potential material applicable to high temperature and low-density refractory for aerospace gas turbines, nuclear constructions and rocket nozzles. Some authors in the literature suggested the addition of several alloying elements to improve the properties of the alloy. Xiaotao *et al.* (2016) considered the effect of adding boron to the $Al_{0.5}CoCrCuFeNi$ HEA using induction melting. The addition of boron led to the strong formation of Cr- and Fe-rich borides in the matrix, which improved the wear resistance and resulted in high compression strength at elevated temperatures. The improvement in the hardness and wear resistance was attributed to the combination of the large hard borides with ductile and tough FCC matrix This shows that the continuous addition of alloying elements further improves the properties of the alloy.

Chen *et al.* (2014), inspected multi-element alloy ($Al_{0.5}CoCrCuFeNi$) prepared by blending various pure metal powders using the MA method and adding different ratios of tungsten carbide to the multi-element alloys. The Tungsten Carbide particles were dispersed homogeneously in the ductile multi-element alloy, forming no second phase. After press forming, the admixed powders were rebound at 500°C and then liquid-phase sintered at 1,300°C–1,450°C. The sintering process of $WC/Al_{0.5}CoCrCuFeNi$ multi-element alloy is like the traditional WC/Co. The hardness of the sintered body of $WC/Al_{0.5}CoCrCuFeNi$ alloy was higher than the traditional WC/Co sintered body measured at room temperature. Its high-temperature hardness was higher than the traditional WC/Co measured at 900°C. Substitution of multi-element alloy for Co as the base phase can enormously improve the material properties of WC super-hard composite material. Yang *et al.* (2017) proposed that the fast cooling rate of the gas atomization process reduces segregation and increases the solid solution strengthening effect of the alloy without reducing its crystallinity. The authors successfully prepared $Al_{0.5}CoCrCuFeNi$, $Al_{0.5}CoCrCuFeNiSi_{1.2}$ and $Al_{0.5}CoCrCuFeNiSi_{2.0}$ HEAs by gas atomization process and the results showed that all alloy powders were spherical shapes with smooth surfaces. Thus, showing that the HEA powders prepared by the gas atomization process, can be used for additive manufacturing (AM) applications.

Madan (2016) investigated the annealing treatment of the induction melted $Al_{0.5}CoCrCuFeNi$ and $Al_{0.5}CoCrCuFeNiMo_{0.25}$ HEAs, which included quenching and normalizing in the furnace. The $Al_{0.5}CoCrCuFeNi$ formed different phases compared to arc melted $Al_{0.5}CoCrCuFeNiMo_{0.25}$ referenced due to inclusions.

The $Al_{0.5}CoCrCuFeNiMo_{0.25}$ had formed copper and molybdenum-rich phases with a minor amount of inclusions or amorphous precipitates. This molybdenum addition had increased the microhardness values. High strain rate testing proved that $Al_{0.5}CoCrCuFeNiMo_{0.25}$ is ductile. The corrosion tests of $Al_{0.5}CoCrCuFeNiMo_{0.25}$ proved that it is nobler than the reference TWIP steel sample in an acidic aqueous solution. However, the authors reported that the $Al_{0.5}CoCrCuFeNi$ via induction cast was very brittle because of the phases observed. Other authors have suggested using alternative manufacturing techniques to further enhance the performance and application of this alloy.

Tang *et al.* (2015b) reported that using an improved fabrication process may enhance the properties of $Al_{0.5}CoCrCuFeNi$ HEA. The manufacturing defects observed attributed to the manufacturing process, brought about the need for innovative and fundamental advances in the manufacturing process of HEAs away from the conventional arc melting and sputtering methods in the literature. The versatility and ability of the AM technique for achieving accuracy and defect-free components are the current forefront of development in advanced manufacturing techniques. In 2013, Yue *et al.* (2013) fabricated the AlCoCrCuFeNi HEA using laser remelting and plasma spraying techniques. The authors stated that microporosity observed in the plasma-sprayed alloy was eliminated after laser remelting resulting in s dense surface. They observed an epitaxial columnar dendritic structure, which was primarily the BCC phase with negligible amounts of FCC phase attributed to the sluggish diffusion effect of the alloy.

The following year, Yue *et al.* (2014) investigated the solidification behaviour of laser deposited AlCoCrCuFeNi HEA on magnesium substrates using Gaumann and Giovanola-Trivedi models. The authors also recorded observing epitaxial crystal structures; however, copper was rejected into the magnesium melt with no alarming dilution occurring on the top layer of the coat attributed to copper's low affinity with other elements. Meng *et al.* (2015) examined the laser surface forming of AlCoCrCuFeNi HEA, which was reinforced with metal matrix composites. The results showed that the tribological features of the HEA were improved with the reinforced particles showing delamination and oxidation wear mechanisms. Copper also segregated to form the Cu-rich phase due to its weak binding with other elements, nonetheless, good metallurgical bonding was observed between the coating and substrate was observed.

Meng *et al.* (2016) studied the influence of copper in the AlCoCrCuFeNi HEA reinforced composite on magnesium substrates via laser melt injection. As expected, copper was rejected, which promoted the BCC phase structure however, the rejection influenced the wear resistance of the alloy negatively attributed to an intermetallic $CuMg_2$ phase observed. Prabu *et al.* (2020) explored the microstructural and wear behaviour of the AlCoCrCuFeNi HEA by laser surface alloying. The results showed that the alloy had a BCC phase with dendritic and interdendritic structures recording a hardness value 3 times higher than the substrate. The alloy also showed improved wear resistance compared to the Ti-6Al-4V substrate attributed to the intermetallic and solid solution mechanism observed. Limited reports are using this advanced manufacturing route in fabricating the $Al_{0.5}CoCrCuFeNi$ HEA, thus limiting the investigation on the fatigue behaviour of the AM HEA.

Huang *et al.* (2018) studied the corrosion and wear resistance of the $Al_{0.5}CoCrCuFeNi$ HEA via laser cladding. The authors reported that the alloy was successfully fabricated on a magnesium alloy substrate, and the results showed that the microhardness of the alloy was more than 3 times higher than its substrate and higher than the arc melted $Al_{0.5}CoCrCuFeNi$ HEA. The alloy also showed better corrosion resistance, proving that an advancement in the manufacturing process of the alloy improves the properties of the HEA.

In recent times, laser surface modification (LSM) has become a cost-effective method used in improving the surface properties of the HEAs by enhancing the amalgam's service life when plagued with poor mechanical, electrochemical and tribological properties which limit its industrial applications. Technological advancements in surface engineering have replaced conventional methods of surface treatments with LSM techniques. The use of lasers in LSM has been reported to produce wear, corrosion, fracture and fatigue resistant HEAs coatings. This is attributed to the energy absorption and rapid solidification of the deposition process, which promotes fine microstructures necessary for surface modification. Wu *et al.* (2017) used laser surface alloying to study the phase evolution and cavitation erosion-corrosion behaviour of a HEA coating in distilled water and NaCl solution. The study showed that the alloy's cavitation erosion resistance was enhanced in distilled water but not in NaCl solution due to corrosion.

Zhang *et al.* (2015) fabricated HEA by laser surface alloying to examine the properties of the alloy, and they reported that the microhardness property of the coating was thrice the number of the substrate and there were improvements in the wear resistance of the alloy. Huang *et al.* (2012) investigated an equimolar HEA on a titanium alloy substrate using LSM and the results also showed enhancements in the wear resistance of the alloy attributed to the manufacturing route which contributed to the formation of the phases observed in the BCC matrix. Nahmany *et al.* (2016) used an electron beam surface remelting technique to modify two–five component HEAs, and the authors inspected the influence of these surface modification processes on the properties of the alloys. The authors observed a significant increase in the microhardness due to the rapid solidification and cooling process associated with the fabrication technique. From literature, it can be deduced that LSM classified into laser surface remelting, surface amorphisation, laser transformation hardening, shock hardening, laser cladding, laser surface alloying and laser shock peening using different lasers can enhance the properties of HEAs (Tian *et al.*, 2005).

2.1 High entropy superalloys

The aerospace industry requires innovative and more efficient high-temperature materials to withstand unfavourable environmental conditions in service and lower emission propulsion for elevated temperature structural applications. The components for gas turbine engines may become hostile due to faster and hotter rotating cores or exposure to environmental conditions that lead to a decline in their mechanical performance. Therefore, these components must

meet the requirements for safe turbine engine operations. The Ni-based superalloy retains some of its properties at high temperatures and the efficiency of the material increases at elevated temperatures. Thus, the material is used for turbine engine structural applications, however, the material has an operational limit at elevated temperatures. Consequently, high entropy superalloys (HESAs) having an atomic ordering and coherent strength as the strengthening mechanisms have been developed as alternative materials to replace conventional superalloys for gas turbine structural applications for enhanced high-temperature oxidation and creep properties (Zhang *et al.*, 2018a).

According to Whitfield *et al.* (2021b), both Ni-based and HESAs contain two crystallographically-related phases, however, the arrangement of their phases and their crystal systems differ and the HESAs have been reported to be 84% cheaper than commercial Ni-based superalloy (Chen *et al.*, 2020). The HESA phase is also based on the ordered BCC system, whilst the Ni-based superalloy has a disordered ductile FCC crystal structure with an ordered $L1_2$ superlattice structure.

Senkov *et al.* (2016) developed $AlMo_{0.5}NbTa_{0.5}TiZr$ HESA and the authors mentioned that the alloy possessed higher compressive strengths and lower densities than the Ni-based superalloys at temperatures between 20°C and 1,200°C. The alloy exhibited two faces; BCC and B2 crystal structure in nanoscale mixtures attributed to the decomposition of a BCC phase at elevated temperatures. Jensen *et al.* (2016) argued that the HESA has a phase separation which explains the microstructural formation mechanism and the chemical interfaces between the two phases; BCC and B2 crystal structures are sharp. Zhang *et al.* (2018a) revealed that the $Ni_{45}(FeCoCr)_{40}(AlTi)_{15}Hf_x$ HESA possesses high ductility and yield strength with no fracture at elevated temperatures attributed to the γ'' particles precipitation strengthening effect. Kong *et al.* (2020) investigated the microstructures and mechanical properties of $Ni_{46}Co_{22}Al_{12}Cr_8Fe_8$ Ti_3Mo_1 HESA fabricated via powder metallurgy. The superalloy's density was lower than conventional Ni-based superalloy at 7.82 g cm^{-3} with an FCC matrix and γ'' particles precipitate, having superior tensile properties than commercial Ni-based superalloy Inconel X-750. The authors stated that the strength of the HESA was improved through dispersion strengthening at high temperatures.

Whitfield *et al.* (2021a) reported that the arrangement of phases in Nickel superalloys and HESAs are very different, the former having a disordered matrix whilst the latter is an ordered B2 phase. However, the continuous ordered matrix phase observed on the grain boundary with intermetallic phases restricts the ductility of the HESAs at room temperature (Senkov *et al.*, 2018a). Soni *et al.* (2018) investigated a novel approach to improving the ductility of the as-cast HESAs through heat treatments at 1,200°C which resulted in an equiaxed grain structure. At 1,400°C the superalloy showed a disordered BCC phase morphologically resembling the γ (FCC) + ordered $L1_2$ phase of the Ni-based superalloy. The authors concluded by reporting a substantial increase in the ductility of the superalloy via annealing. The heat treatment successfully inverted the ordered B2 phase into a ductile disordered BCC phase. Nonetheless, additional studies on the thermal stability of HESAs at several service temperatures are required to understand the interaction between the microstructure, phase equilibria and the mechanical properties of the superalloys at elevated temperatures.

Gorsse *et al.* (2021) analysed the hierarchical microstructure kinetics of HESA using computational thermodynamics to reproduce the origin and evolution of the experimental microstructures during thermal treatments. The authors listed the composition of HESAs to contain principal elements such as Al, Ti, Nb, Ni, Co, Cr, Fe, Mo and W. Isothermal ageing treatments at 1,023 k for 20 h with water quenching promotes the development of the hierarchical microstructure nonetheless, lowering the ageing temperature and increasing the ageing time was suggested to attain elevated temperature tensile strength (Meher *et al.*, 2018). The authors concluded that kinetic tools and computational thermodynamics can be used to predict the precipitation processes of HESAs; however; the improvement of HESAs is dependent on the phase equilibria.

Saito *et al.* (2021) studied the tensile creep behaviour of HESAs at intermediate temperatures or turbine blades applications. For a typical flight cycle in the aerospace industry, less time is spent on the maximum thrust and more time is spent on minimal severe cruise conditions; therefore, most turbine engine components spend their service life at intermediate temperatures. The authors claimed that HESAs creep deformation mechanism in the range of 500 MPa and 600 MPa at 760°C is independent of the applied stress. The bypass and climb motion of dislocations, which were the major deformation mechanisms, were not influenced by the secondary γ'' precipitates. The creep condition at 760°C was selected to reduce the degree of coarsening because the γ'' precipitates were reported to change its original microstructure at 870°C furthermore, reports on the B2 becoming unstable at temperatures higher than 900°C eliminates the order hardening as the strengthening mechanism at elevated temperatures (Whitfield *et al.*, 2020). These limitations also apply to Ni-based superalloys as studies on the creep conditions of Ni-based superalloys in literature have been carried out at 774, 750 and 760°C. Chen *et al.* (2020) reported that data from the literature on the mechanical properties of the alloys are from compression tests or tensile tests at intermediate temperatures and limited studies have been done on irradiation, fracture toughness, tribology and oxidation properties of these superalloys at elevated temperatures.

2.2 High entropy films

The aerospace industry has experienced the evolution of film components through microelectromechanical systems (MEMS) attributed to their reliability and size. Nonetheless, these films are constantly subjected to fatigue damage which is the common failure node for film materials under cyclic loading. Therefore, the demand for films to possess hardness and fatigue resistance without any tradeoffs has sparked the development of high entropy film materials to surpass the properties of conventional brittle Cu, TiNi, AlN, ZnO, TiN, CrALTiN, TiAlN films available (Wang *et al.*, 2020b). According to Yan *et al.* (2018b), high entropy films are prepared by chemical or physical vapour deposition (PVD) methods. Physical fabrication of films is achieved via ion plating

(Ikeda and Satoh, 1991; Uchida *et al.*, 2004), vacuum evaporation (Heavens, 1950; Klenk *et al.*, 1993; Kumar *et al.*, 2003), sputtering (Mittmann *et al.*, 2019; Yan *et al.*, 2018a) and cladding (Contin *et al.*, 2017; El-Bashir *et al.*, 2019) whilst chemical methods include liquid phase deposition (Bianchi *et al.*, 2017; Zalden *et al.*, 2019; Zhang *et al.*, 2020). The authors stated that laser cladding and magnetic sputtering are the most significant fabrication routes (Xing *et al.*, 2019). Dolique *et al.* (2009) mentioned that using magnetic sputtering with multiple targets is an efficient way to control the composition of films by adjusting each target. The CoCrFeMnNi system, unlike other HEAs at low temperature, exhibits good strength, fracture toughness and ductility, making it a potential material for MEMS. However, the alloy has low yield strength at room temperature (Wang *et al.*, 2020c). Therefore, the modification of the alloy to improve its properties has been investigated; thus CoCrFeMnNi alloy was prepared via magnetic sputtering with ultrahigh-density nano twins and the HEA films (HEAFs) were reported to exhibit higher hardness-fatigue resistance with no tradeoffs through strain hardening and the dissipation of detwinning with twin spacing at 2 nm or more (Wang *et al.*, 2020b). High entropy films due to the high entropy effect influence high strength and fatigue resistance, making the material a potential substitute for conventional film materials (Tang *et al.*, 2015a; Yang *et al.*, 2018).

Fang *et al.* (2020) proposed using elemental strengthening effects to modify the properties of the HEAFs and the authors examined the influence of V on CoCrFeMnNiV_x HEAFs via magnetron co-sputtering. The films with the FCC phase had excellent ductility attributed to the nano twins and nanograins observed. The transformation from an FCC phase to an amorphous phase occurred as the V content increased and the strain hardening effect attributed to the presence of nano twins was abundant at low V contents (Salishchev *et al.*, 2014). He *et al.* (2014) investigated the influence of Al on the FeCoCrMnNi HEAs via arc melting, which showed a change in structure from FCC to Bcc as the Al concentration increased (HsuLi and Hsueh, 2020). However, in the FCC region, the alloy had good ductility with a trade-off with its strength. At the region where both FCC and BCC phases were observed, the alloy showed increased strength with a trade-off with its ductility, whereas at the region where only the BCC phase was observed, the alloy was extremely brittle (Brechtl *et al.*, 2019).

Cheng *et al.* (2019) proposed improving the strength of the FeCoCrMnNiAl_x alloy by sintering after MA and the authors reported an improvement in the strength of the alloy attributed to the BCC precipitation and fine grains without trade-off with its ductility but its plasticity. Qin *et al.* (2019a) attempted to add Mo to the CoCrFeMNNi system which resulted in the formation of a sigma phase and improvement in compressive yield strength attributed to the phase formation and solution strengthening effect, however, there were no reports on the hardness properties. On the other hand, Wang *et al.* (2019a, 2019b, 2019c, 2019d, 2019e) proved that doping the CoCrFeMnNi compositional system with Nd resulted in the strengthening of the alloy with good ductility through precipitation hardening which occurred randomly inside the grains and at the grain boundaries.

Over the years, nitride films have become more and more popular due to their high strength, wear resistance, hardness and tensile strength. Cui *et al.* (2020) fabricated (ALCrTiZrHf) N HEAFs via reactive magnetic sputtering and the alloys exhibited an amorphous state, however, with an increase in the flow rate of N_2, the phase transformed to an FCC structure. The solution strengthening effect and the saturated metal-nitride phases observed were responsible for the strengthening effect of the films. The films also exhibited superior wear resistance with a relatively low friction coefficient and good ductility, making them suitable for protective coatings in aerospace applications. Chen *et al.* (2004) also explored the changes in the phase structure of FeCoNiCrCuAlMn films with a change in the nitrogen flow rate using reactive sputtering and the nitride films showed an amorphous nature as the gas flow rate of nitrogen increased. The authors varied the substrate bias and the nitrogen partial pressure parameters to examine the influence of these variables on the properties of the films. Although Xing *et al.* (2019) reported that substrate bias affects the corrosive resistance, the elastic modulus and hardness properties, the results showed that the property of the films was not affected by the substrate bias attributed to the amorphous phases observed in the FeCoNiCrCuAlMn film.

Huang *et al.* (2007) gave insights into the $Al_{0.1}$CoCrFeNi HEAFs prepared by magnetic co-sputtering and investigated their size-dependent mechanical properties. It was found that the stacking faults attained high hardness with an increase in the grain size of the films and vice versa attributed to the stacking fault and grain boundary strengthening mechanism. However, the strain rate sensitivity decreased with an increase in the grain size. The authors proposed that HEAFs deposited on a three-dimensional micro or nanolattice scale result in improved mechanical properties without any tradeoffs. Nonetheless, manipulating the internal microstructures by decreasing the grain size of the HEAFs has proven to be more effective (Jiang *et al.*, 2020). Khan *et al.* (2020) prepared AlCoCr$Cu_{0.5}$FeNi HEAFs using magnetic sputtering and they discovered that the thin films are potential materials for engine blades and turbines applications. Whilst Wang *et al.* (2020a) mentioned that the Al_xCoCFeNi HEAFs system can be used as thin-film resistors in the aerospace industry attributed to the little temperature coefficient of resistance they possess and their high accuracy of resistivity.

2.3 High entropy bulk metallic glass

In 1960, Klement Willens and Duwez (1960) during the fast quenching of gold-silicon alloys discovered bulk metallic glasses (BMGs) whilst studying the non-crystalline structures of the $Au_{75}Si_{25}$ alloy. In recent times, BMGs are used as engineering materials in the aerospace industry attributed to their high damage tolerance, corrosion and wear resistance, biocompatibility, strength and yield strength attributed to their disordered atomic structures (Ashby and Greer, 2006; Trexler and Thadhani, 2010). Haratian (2020) proposed using BMGs as debris shielding components to face high impact velocity in the aerospace industry. Nonetheless, the material's intrinsic brittleness, micro-cracks and high viscosity attributed to the manufacturing route limit the application of these materials (Zou *et al.*, 2020). These defects are observed when BMGs do

not maintain their amorphous structures when the manufacturing process has insufficient cooling rates (Sohrabi *et al.*, 2021).

According to Gao *et al.* (2011), BMGs are made up of principal elements, Cu, Fe, Mg and Zn until recently when more than five principal elements were combined to form a series of high entropy BMGs. High entropy BMGs (HE-BMGs) is HEAS obtained with the amorphous structure resulting in a glassy formation as opposed to the simple FCC, FCC + BCC or BCC phases most HEAs structure have. The mixing enthalpy between the elements, the atomic size between them and the high cooling of the fabrication process, are the most important factors to consider when preparing HE-BMGs (Wang *et al.*, 2004). $Pd_{20}Cu_{20}Ni_{20}P_{20}$, $Ti_{20}Zr_{20}Hf_{20}Cu_{20}Ni_{20}$ and $Zn_{20}Ca_{20}Sr_{20}Yb_{20}(Li_{0.55}Mg_{0.45})_{20}$ are all HE-BMGs with relatively close atomic sizes and good mixing enthalpies fabricated by a rapid cooling method (Ma *et al.*, 2002; Zhao *et al.*, 2011).

Notably, AM is a state-of-the-art process widely reported to have rapid cooling and solidification thermal cycles without the constraint of the thickness or size of the components, unlike conventional fabrication techniques (Frazier, 2014; Thampy *et al.*, 2020). Zheng *et al.* (2008b) established the cooling rates of laser engineering net shaping, an AM technique, using dendrite arm spacing. The authors reported that the cooling rates are between 10^3 K/s and 10^4 K/s whilst the cooling rates of the selective laser melting (SLM) process were reported to be at 10^4 K/s (VilaroColin and Bartout, 2011; Zheng *et al.*, 2008a). The rapid cooling rates of the AM technique is attributed to the rapid prototype-assisted conformal cooling channels associated with the AM process. Compared with conventional cooling channels that are machined in straight lines, thereby producing uneven cooling across the HE-BMGs fabricated, leading to warpage, scrap, longer cycle times and uneven cooling (Shinde and Ashtankar, 2017). Consequently, the AM process has become a recent option for the production of HEA-BMGs asides from powder metallurgy with complex large geometries that do not crystallize with excellent glass-forming abilities (Tong *et al.*, 2019) and increase in thickness as reported by Xu *et al.* (2019), KumarDesai and Schroers (2011), Schroers (2010).

Li *et al.* (2020) prepared FeCoCrNiMn HEA metallic glass via SLM and the authors reported the HEA-BMGs having high thermal stability, strength at 1,000 MPa and toughness over 100 MPa $m^{1/2}$. Shu *et al.* (2018b) studied the FeCoCrBNiSi HEA-BMGs via laser cladding, investigating the effect of the Fe:Co ratio on the glass forming ability (GFA). The results showed that specimens with the lowest Fe:Co ratios of 1:1 showed the highest microhardness and elevated temperature wear resistance attributed to the high amorphous content whilst an increment of the ratios weakened the GFA of the HE-BMGs (Shu *et al.*, 2018a).

Cheng *et al.* (2020) doped $Fe_{25}Co_{25}Ni_{25}$ $(B_{0.7}$ $Si_{0.3})_{25}$ HEA-BMGs with Nb to examine the influence of Nb on the microstructure and wear behaviour of the coatings using micro strain. The results confirmed amorphous structures with high hardness, wear-resistance and GFA at 2% Nb content. However, as the Nb content increases, the amorphous phase becomes a (Fe, Co, Ni) $_2$, BCC, FCC and Laves phase. Cao *et al.* (2018) proposed improving the GFA of HEA-BMGs through oxygen microalloying and the results showed that the addition of small atoms of oxygen-enhanced the GFA of Zr_{20} Cu_{20} $Hf_{20}Ti_{20}Ni_{20}$ HEA-BMG although the metallic glass was prepared using arc melting. Best *et al.* (2020) reported that the low fracture toughness in $Zr_{59.3}Cu_{28.8}Nb_{1.5}Al_{10.4}$ HEA-BMG is a result of higher dissolved oxygen fabricated via laser powder bed fusion. The authors explained that porosity found is a processing defect associated with the laser AM technique when the process is not fully optimized. These defects can lead to a loss in the mechanical properties of HEA-BMG. More studies using laser AM are yet to be fully explored.

2.4 High entropy ceramics

High entropy ceramics (HECs) are materials with four or more distinct anion and cation sublattices (OsesToher and Curtarolo, 2020; Wright and Luo, 2020; Zhang and Reece, 2019). They contain single phases with multiple elements, adjustable properties and a large compositional space which can be used as insulators and semiconductors with structural diversity (Sharma *et al.*, 2018; Wen *et al.*, 2020). These materials were initially investigated as thin films by using magnetron sputtering in an argon and nitride atmosphere, resulting in an amorphous phase. Until Lai *et al.* (2006) prepared and characterized an AlCrTaTiZr nitride coating using reactive radio-frequency magnetron sputtering which resulted in a single-phase crystalline structure as opposed to a multiphase film with an amorphous structure. Rost *et al.* (2015b) also reported fabricating $(Co_{0.2}Cu_{0.2}Mg_{0.2}Ni_{0.2}Zn_{0.2})$ O stabilized oxide. Thus, HECs have several chemistries such as borides, nitrides, oxides, silicide and carbides with applications as thermoelectric supercapacitors (Jin *et al.*, 2018; Lu *et al.*, 2014; Zhang *et al.*, 2018b), lithium-ion batteries (Qiu *et al.*, 2019; Wang *et al.*, 2019b), microelectronic diffusion barriers (ChangChen and Chen, 2009; Chang *et al.*, 2013), corrosion, biocompatible and wear-resistant coatings (Braic *et al.*, 2012a; Braic *et al.*, 2012b; Lin *et al.*, 2010), catalysis (Chen *et al.*, 2018a; Chen *et al.*, 2019), spintronic layers and thermochemical water splitting (Zhai *et al.*, 2018). (MgCoNiCuZn)O rock salt single-phase HECs have been fabricated via nebulized spray pyrolysis, flame spray pyrolysis, reverse co-precipitation and solid-state reaction (Sarkar *et al.*, 2017a; Bérardan *et al.*, 2016; Rost *et al.*, 2015a).

Copper was reported to be the most anomalous cation in the rock salt formation with a disruptive role in the lattice of the HECs (Anand *et al.*, 2018; OsesToher and Curtarolo, 2020). Cu forms Bragg peak intensities, shapes and width which deviates from the rock salt structures and also has a tendency to separate phases into tenorite CuO and Cu_2O at $\leq$ 800°C and $\geq$ 1,100°C, respectively, and at different quenching conditions and heat treatments (Berardan *et al.*, 2017; Diercks *et al.*, 2017; Meisenheimer *et al.*, 2019). Ye *et al.* (2019) fabricated $(Zr_{0.25}Nb_{0.25}Ti_{0.25}V_{0.25})C$ HEC via hot pressing sintering and the results showed that the HEC had a rock salt crystal structure alongside nanoplate structures with nanoscale to microscale compositional uniformity. The HEC had a relative density of 95.1%, however; it showed low thermal conductivity when compared with other metal carbides at room temperature attributed to the nanoplates, solid solution phase and porosity. Single-phase fluorite oxides having three to seven cations were fabricated using stoichiometry with rare earth

elements (Chen *et al.*, 2018d; Gild *et al.*, 2018; Sarkar *et al.*, 2017b). The (HfZrCeTiSn) O_2 HEC showed entropy stabilization which has a reversible transition from a multiphase to a single-phase and vice-versa when annealed at lower temperatures (Wright *et al.*, 2020). Accordingly, the fluorite oxide prepared via spark plasma sintering (SPS) showed a high annealed density of 100% (Gild *et al.*, 2018; Wright *et al.*, 2020). On the other hand, based on the C40 crystal and hexagonal structures, (MoNbTaTiW)Si_2 and (MoNbTaWZr)Si_2 high entropy silicide synthesized via SPS have very low symmetry structures (Gild *et al.*, 2019; Qin *et al.*, 2019b) whilst high entropy diborides fabricated via SPS have a hexagonal AlB_2 structure with densities greater than 92% having a quasi-two-dimensional high entropy metal layer without segregations and excellent oxidation resistance (Gild *et al.*, 2016; Mayrhofer *et al.*, 2018).

2.5 High entropy steels

The lattice distortion effect enables HEAs to possess excellent hardness, however; this is usually at a trade-off with the ductility of the alloy. Therefore, high entropy steels (HES) were investigated to exploit the flat configurational entropy of transitional metal mixtures with interstitial elements of non-equiatomic compositions. Raabe *et al.* (2015) fabricated quinary FeMnAlSiC HES, which showed low and high-temperature ductility, strain hardening and strength with a 17% reduction in its mass density. Adjusting the stacking fault energy can adjust the microstructural stability of the HES. The interstitial element C notably helped with the stabilization of the FCC solid solution phase and positively influenced the valence electron concentration (VEC) of the HES. Where the rule states the VEC has to be ≥ 8 to form a stable FCC phase, the Fe has a VEC of 8, Al has a VEC of 3, Mn has a VEC of 7 whilst Si and C has a VEC of 4 suggesting that interstitial elements like C and N which has a VEC of 5 can be used to form FCC solid solution phases (Guo *et al.*, 2011).

Jain *et al.* (2020) prepared a non-equiatomic $Fe_{40}Mn_{14}Ni_{10}Cr_{10}Al_{15}Si_{10}C_1$ HES via MA and SPS. The HES had a density of 6.8 g/cm^3 with a single nano-crystalline BCC solid solution phase after milling for 40 h, with an average particle size of 8 to 10 μm which transforms to an austenite FCC + B2 and $Cr_{23}C_6$ phase after SPS. The HES had Vickers hardness of 596 HV with a 1.7 x 10^{-8} mm^3/m wear loss rate was recorded. The authors concluded that more studied on the wear resistance of the HES should be reported because there are limited reports on the HEA steel in the literature.

2.6 High entropy polymer

The HEA concept has been used to create novel materials for several applications. High entropy polymers (HEPs) are a new class of materials that uses a solvent to make several polymer compositions, thus the polymer compositional mixes and the entropy of mixing decreases in linear proportions which is weakened for large polymer molecules. The possibilities of mixing five or more different polymers species into thin films were explored using spin coating via a common solvent by HuangYeh and Yang (2021). The authors selected five different polymers; poly (methyl methacrylate), polystyrenes, polyvinylpyrrolidone and polycarbonate at room temperature into thin films by spin coating on a glass slide. They investigated the effect of polymer miscibility on the de-mixing of the blends by replacing poly (methyl methacrylate) with poly (2, 6-dimethyl-1, 4-diphenyl oxide). The results showed that the heterogeneous domain size Λ observed in most polymer blends can be suppressed with an increase in the number of polymer species in the blend which is attributed to kinetic steric blocking and high entropy mixing. The Λ distribution was random and independent of each polymer species which suggests that the blend is not influenced by the enthalpy interactions between the polymer species (HuangYeh and Yang, 2021).

3. Advances in manufacturing technology

Over the years, the conventional manufacture of HEAs is through induction or arc melting (Jablonski *et al.*, 2015). However, the machining of the final parts produced through these fabrication routes is difficult, expensive and results in material waste whilst extensive heat treatments are required to get the desired properties (Eißmann *et al.*, 2017). Therefore, AM could be an alternative manufacturing route. AM produces near-net-shape components with geometric complexities (Herzog *et al.*, 2016). The freeform fabrication process is achieved layer-by-layer, thereby reducing waste and density, making it cost-effective (Emmelmann *et al.*, 2013). There are diverse AM technologies with the same operational approach, namely; powder bed fusion, direct energy deposition, material extrusion, sheet lamination, binder and material jetting (Wong and Hernandez, 2012). The process starts with a three-dimensional, computer-aided design model on a computer and is generated by reverse engineering.

The CAD model is sliced into layers virtually with different thicknesses depending on the AM technology (Gebhardt, 2011). The data derived from this design is used to produce the components repetitively by a heat source, either through a laser or electron beam (Yan and Yu, 2015). AM spherical powder production for excellent flowability characteristics includes water, plasma or gas atomization, metallothermic, hydride-dehydride and electrolytic processes (Qian and Froes, 2015). Although water atomization may not be suitable for reactive metals, using different powder production techniques results in diverse chemical compositions, particle sizes and morphologies. Oxidation in gas atomization is reduced by using inert gases; consequently, the type of gas used also influences the AM powder phase compositions (Starr *et al.*, 2012).

3.1 Laser surface modification of high entropy alloys

HEAs have characteristic high entropy mixing, sluggish diffusion, lattice distortion and cocktail effect contributing to the alloy possessing outstanding properties, however, influenced by the manufacturing processes (Emmelmann *et al.*, 2013). According to the literature, HEAs are usually prepared by casting attributed to the low porosity, energy and time consumption associated with the technique (Alshataif *et al.*, 2019). Nonetheless, the as-cast HEAs have been reported to have lower strength compared to other fabrication techniques (Qin *et al.*, 2020). Zhang *et al.* (2012b) fabricated AlCoCrFeNi HEA via Bridgman solidification and copper mould casting to investigate the influence of the fabrication technique on the alloy and the results showed that the alloy possessed the same BCC phase with the two methods, however, the alloy produced

via Bridgman solidification showed excellent plasticity compared with the as-cast alloy attributed to the external plastic deformation, low-angle grain boundary, less dislocation motion and pile up whilst the absence of defects contributed to the release of stresses (Ma *et al.*, 2014).

PraveenMurty and Kottada (2013) fabricated HEAs via SPS and the authors stated that the alloy's hardness was five times more than the as-cast HEAs whilst the yield strength was three times more than the traditional casting method. Rogal *et al.* (2017) produce CoCrFeMnNi HEAs via hot-isostatic pressing, the compressive yield strength of the alloy increased four times more than the as-cast alloy. The AlCrCuFeTiZn HEA fabricated via vacuum-hot pressing technique possessed a BCC solid solution phase with high strength and hardness than the as-cast HEA (VaralakshmiKamaraj and Murty, 2010). Zhu *et al.* (2018) fabricated CoCrFeNiMn HEA via SLM and the authors described the alloy as having tensile yield strength twice that of the traditional cast HEA.

Dada *et al.* (2020) fabricated AlCoCrFeNiCu and AlTiCrFeCoNi HEAs via laser melting deposition (LMD). The alloys showed transitional columnar and equiaxed dendritic structures, respectively, shown in Figure 2, with FCC, BCC phases and a small amount of intermetallic phase in the AlTiCrFeCoNi contributing to the increased hardness of the alloy. Haase *et al.* (2017) also fabricated HEA via LMD and the alloy exhibited compressive yield strength higher than conventional casting techniques attributed to the texture of the alloy, the rapid cooling and the solidification process (Zhang *et al.*, 2012; Brif *et al.*, 2015).

Figure 2 Microstructure

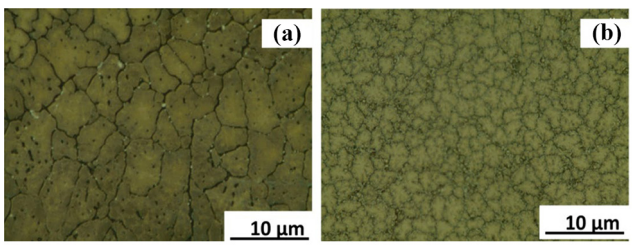

Notes: (a) AlCoCrFeNiCu; (b) AlTiCrFeCoNi HEA via laser AM (Dada *et al.*, 2020)

Surface coatings are classified into metallic, composite and ceramic coatings and fabricated through laser deposition, vapour deposition, powder metallurgy and thermal spraying with post-treatments such as annealing, friction stir processing and laser remelting (Li *et al.*, 2019). In aerospace applications, the surface of HEAs are subjected to external stimuli and a poor surface-related properties such as oxidation, wear, corrosion and fatigue will reduce the performance of the alloy during service., therefore, the study of surface modification techniques that retains the material's properties whilst modifying the surface to improve its properties, is of great importance to reduce material degradation and improve the performance of HEAs (Baburaj *et al.*, 2007). Laser processing stabilizes the HEA phase structures attributed to the rapid cooling and solidification rates that restrict diffusion, nucleation and growth of intermetallic compounds at elevated temperatures (Ocelík *et al.*, 2016).

3.1.1 Laser ablation

Krasnov (1973) first reported on laser ablation which is a process of surface modification generating micro columnar arrays by increasing the bond strength within the alloy thus improving the adhesive bond strength, the surface area and the wettability of the interface of the HEAs (Baburaj *et al.*, 2007). This process is shown in Figure 3, can ablate any type of solid sample without sample preparation or size requirements, making the technique a very straightforward and simple process. A laser beam is focused on the sample surface and converts a finite volume of the sample surface to vapour phase constituents and then the vapour converted is analysed by measuring the atomic emission in induced plasma by transporting the vapour inductively to coupled plasma (Russo *et al.*, 2002).

Figure 3 Schematic diagram of laser ablation (Chatterjee and Deopura, 2002)

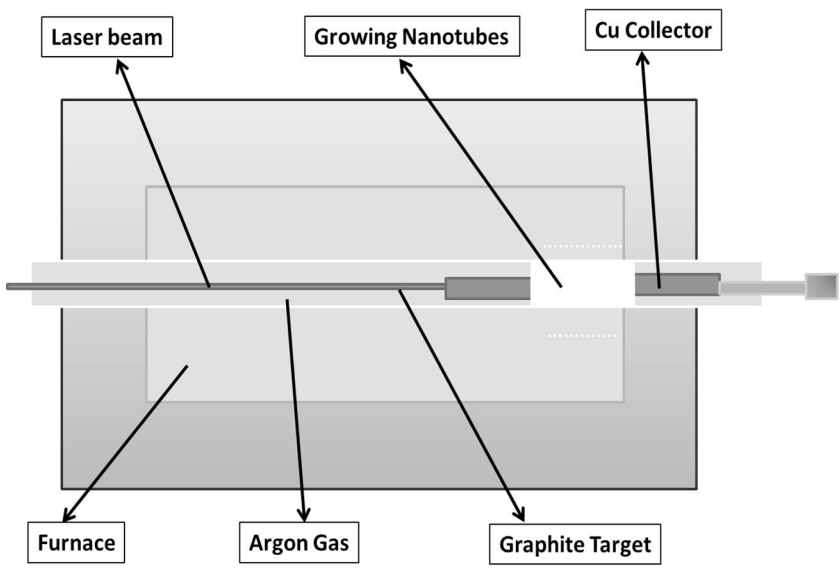

Wang *et al.* (2019a) used picosecond-pulsed laser ablation in fabricating colloidal HEAs nanoparticles instead of the conventional carbothermal shock technique producing only nanoparticles immobilized on surface-oxidized and conductive carbon materials, thereby limiting its application. The results showed that the colloids of isolated HEA nanoparticles produced were highly stable based on the reduced deviations of catalytic performance of the HEA nanoparticles. Redka *et al.* (2021) used laser ablation at a wavelength of 1,056 nm and a pulse duration of 530 fs to fabricate CrMnFeCoNi HEA. HEAs have been reported to show damage resistance to a high level of energy particle irradiation attributed to its configurational entropy. Therefore, the authors used laser as a means to interact with high energy electromagnetic radiation, comparing the results from the HEA with that of stainless steel AISI 304, which has been extensively studied in the literature. The results showed that the HEA had a higher ablation volume but a lower damage threshold than steel. The authors argued that there is a gap in knowledge regarding subtractive laser fabrication of HEAs and recommended ultrashort-pulse lasers as an efficient laser micro-machining route for HEAs, as the configurational entropy of the HEA does not influence on the damage behaviour of the ablation process.

3.1.2 Laser microfabrication

This LSM technique, shown in Figure 4, involves the fabrication of materials in the micrometre or miniature components applied in engineering with low manufacturing costs and higher precision (Alemohammad, 2010; Piqué and Serra, 2018).

Dong *et al.* (2018) made an octet micro lattice metallic mechanical metamaterials using a low-cost microfabrication technique compared with conventional methods such as SLM, snap-fit techniques, electron beam melting, investment casting and brazing. These microfabrication methods have been used to develop other materials used for aerospace applications, but limited studies are based on the use of these techniques for fabricating HEAs (Li *et al.*, 2008; Rötting *et al.*, 2002). Liao *et al.* (2017) detailed that $CoCrFeNiAl_{0.3}$ HEA thin-film coating can be processed using advanced coating techniques and microfabrication methods. The AM of micro lattice materials is challenged with the lattice strut diameter produced with decreased metal particle diameters, which results in high surface roughness, chemical inhomogeneity and internal defects. However, microfabrication methods such as lithography, bonding, electrical induced nanopatterning, photolithography, colloidal monolayer and rapid prototyping are current advances in the microfabrication methods for miniature and portable components (VoldmanGray and Schmidt, 1999).

3.1.3 Laser surface micro-texturing

This advanced technique shown in Figure 5 is applied on the surface of a material to improve adhesion, wettability and the corrosion resistance of materials, thus reducing wear and friction with application in the aerospace, biomedical and automobile industries (Mezzapesa *et al.*, 2013). LSM texturing manufactures dies and moulds, improves osseointegration and controls cell responses which enhance the fixation of implants in the bone, thereby needs to be a future research focus (Etsion,

Figure 5 Schematic diagram of laser surface micro-texturing (Mezzapesa *et al.*, 2013)

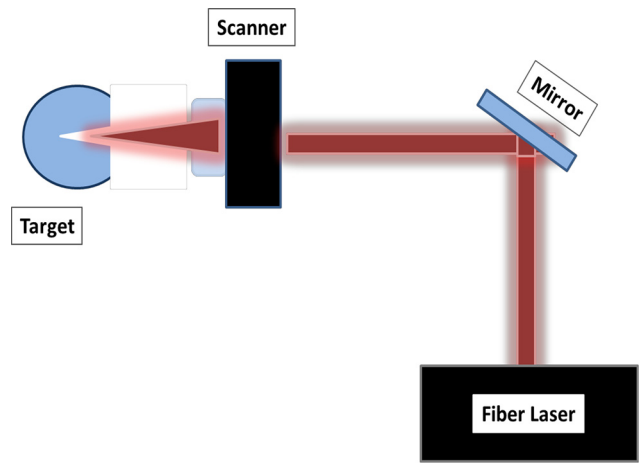

Figure 4 Schematic diagram of laser microfabrication (ZhangMen and Chen, 2011)

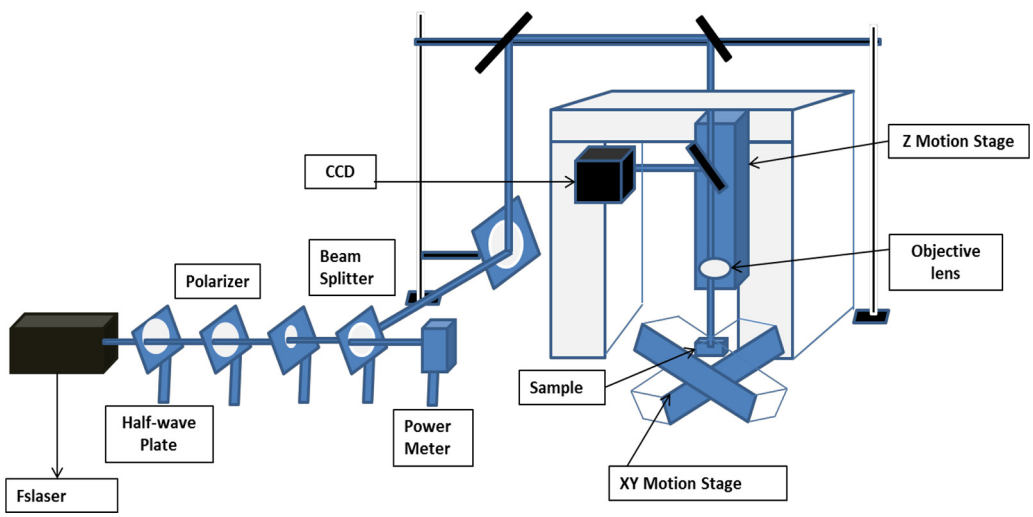

2005; Mirhosseini *et al.*, 2007; Vilhena *et al.*, 2009). Surface texturing results in enhanced tribological properties and load capacity (Pratap and Patra, 2018). It is used to produce a high number of micro-dimples serving as a hydrodynamic bearing on the material surface and liners for combustion engines (Etsion, 2005). Advances in surface micro texturing generate a surface texture with excellent machining repeatability, which can also fabricate micro features on the surfaces of metals, thus requiring a sustainable technology that does not change the initial properties of the metal (Kobayashi and Shirai, 2008). The term "texturing" is a unique way to change the surface properties of materials' defining surfaces that contain micro patterns, holes, hairs, dimples and asperities (PatelJain and Ramkumar, 2018). Ball (1999) studied the reduction of drag in aerospace by applying a microscopic texture with a transparent plastic film. The results showed that the riblets were the same texture as shark skin, decreasing drag by 8% and resulting in fuel conservation.

3.1.4 Laser nanofabrication

This method is a flexible setup operated in a vacuum, air or liquid environment and applied in imaging, biological sensing, therapeutics, optoelectronics and photovoltaics. The process shown in Figure 6 is a surface modification technique that needs widespread research for HEAs' commercialization purposes (Sekkat and Kawata, 2014; Sun *et al.*, 2003). Advances in this technique use an ultrafast laser that alters the properties of materials and control materials for micro to nanometer-scale fabrication (Gattass and Mazur, 2008). Gattass and Mazur (2008) mentioned that advances in laser nanofabrication include the use of femtosecond lasers that breaks the limitations of conventional fabrication methods by improving the quality of the fabrication, reducing heat-affected zones, recast layers and cracks (Xiao *et al.*, 2018). Kim and Kim (2019) used a thermal plasma jet as a nanofabrication technique to ease against high selectivity regarding the scalable production of materials, a specific morphology or chemical composition. The authors detailed that the fabrication process resulted in high purity, throughput and anisotropy. Nanoscale HEAs consist of five or more elements in nanoscale proportions fabricated to produce plasmonic behaviour, super magnetic and superconducting properties. These materials are stabilized by their high configurational entropy; however, their composition as a single nanoparticle is very difficult to maintain, which has led to the formation of intermetallic nanoparticles with defined crystal structures and stoichiometry. Therefore, rapid quenching is recommended via thermal plasma jet (Yao *et al.*, 2018).

3.1.5 Laser shock peening

This manufacturing process shown in Figure 7 involves the subjection of a surface to laser shocks using a high energy laser. The peening process starts when a laser beam with high energy hits the surface of the component, and a plasma shock wave applies a high amount of pressure to the same surface, thus reshaping the microstructure of the component. The distorted metal with a plastically deformed section pushes up against the surrounding structures, which adapts to the enlarged volume of metal that was affected by the laser peening. Having a versatile, non-contact and robust characteristic above other laser surface treatments and limiting the surface treatment to specific areas of need, the robotic arm of the equipment can deliver the laser shock separately by manipulating the robotic arm. Reports in literature also show that simultaneously shocking the sides of a material increase the hardness of materials, due to cold working from superpositioning of the opposite shocking (Ding and Ye, 2006). The yield strength, corrosion and fatigue resistance of materials have also been reported to be enhanced using laser shock peening (Clauer, 1996). To help commercialize the process for industrial purposes, it is important to build a laser system with pulse frequency and small footprint with enough energy at a reasonable cost to demonstrate that LSP is a viable process in the surface treatment of HEAs especially in mitigating fatigue-related problems (Zhang *et al.*, 2010).

3.1.6 Laser pulse deposition

In a laser pulse deposition technique, an ultra-short laser pulse causes the deposition of laser energy in extremely thin layers of the component, thereby producing a high-density plasma that is relaxed by plasma expansion, radiative transport, shock and

Figure 6 Schematic diagram of laser nanofabrication (Mezzapesa *et al.*, 2013)

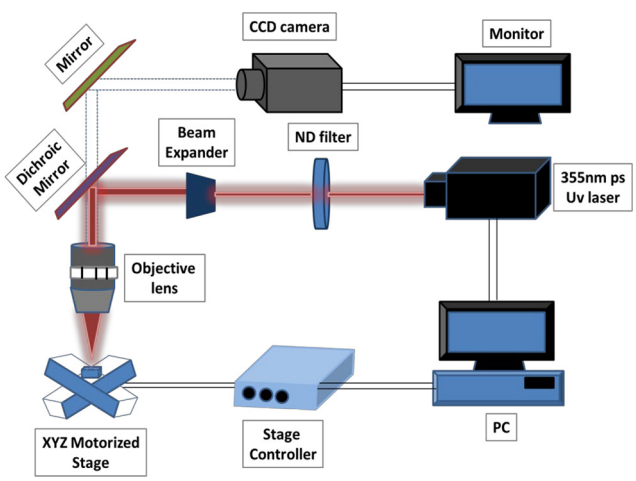

Figure 7 Schematic diagram of laser shock peening (Mathew *et al.*, 2021)

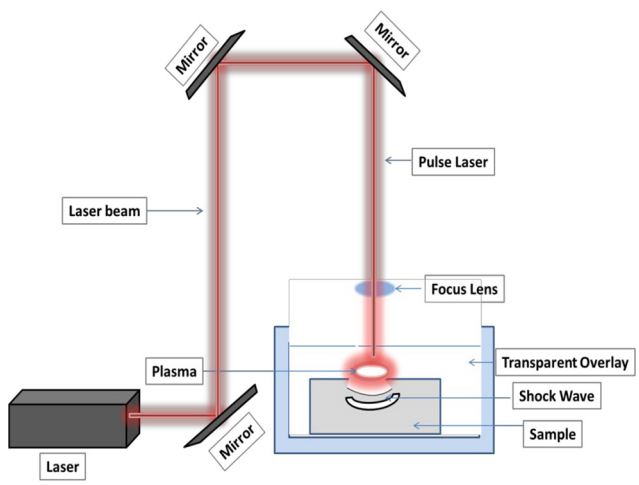

wave generation, thus ensuring the reduction of collateral damage (Rubenchik *et al.*, 1998). The deposition shown in Figure 8 via an electronic process joins the material with photonic energy whilst a laser pulse focused on the target goes through an optical window of an empty chamber. This results in material removal at a certain power density occurring as ejected luminous plume. However, the target material determines the threshold power density required to produce the plume (Willmott and Huber, 2000). Lu *et al.* (2019b) fabricated high entropy thin films (HEASTFs) using laser pulsed deposition and, the results showed that the thin films had higher nanohardness and lower elastic modulus than the bulk alloy with lower corrosion resistance than 3,161 stainless steel, thus making it a potential advanced technique in processing HEATFs.

3.1.7 Laser friction stir deposition

Phillips *et al.* (2019) defined additive friction stir deposition as a solid-state process that avoids deleterious effects such as porosity, cracking and other defects without post-processing. Metallic powders are forced through a non-consumable rotating cylindrical tool whilst the tool generates pressure and friction heat alongside severe plastic deformation on the subsequent layers of the material and the substrate which initiates dynamic recrystallization resulting in the refined microstructure of the component produced. Shukla *et al.* (2020) developed a novel solid-state gradient friction stir alloying technique for exploring transformation induced plasticity in HEAs (Agrawal *et al.*, 2020). The method shown in Figure 9 had a tampered region of the alloying element added in the base alloy groove through milling. As the friction stir process continued, the additional alloy content increased. The authors studied the mechanical properties of the HEA and the gradient distinctions of copper in the phases (Wang *et al.*, 2019a). The results showed that an increase in the copper content promoted grain refinement, stabilized the gamma microstructure and increased the phase fractions whilst the HEA also showed an increase in mechanical properties. According to Li *et al.* (2019), friction stirring processing can be used as a post-treatment whilst Yang *et al.* (2020) used a friction stir process to fabricate a 5,083 Al matrix composite reinforced with HEA particles. Advances in additive friction stir deposition are associated with the fourth industrial revolution where three-dimensional printing, rapid prototyping and freeform fabrications are key elements to a promising alternative to metal and laser AM processes (GopanWins and Surendran, 2021).

Figure 8 Schematic diagram of PLD (Lu *et al.*, 2019)

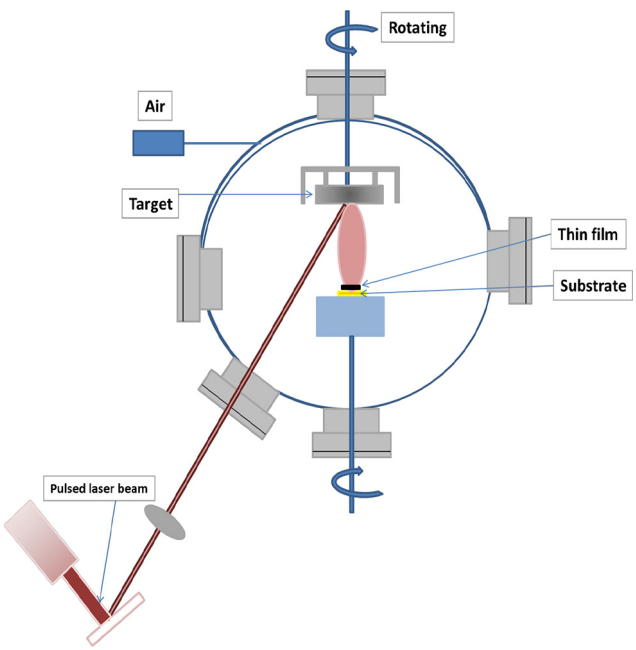

Figure 9 Schematic diagram of friction stir deposition (PalanivelSidhar and Mishra, 2015)

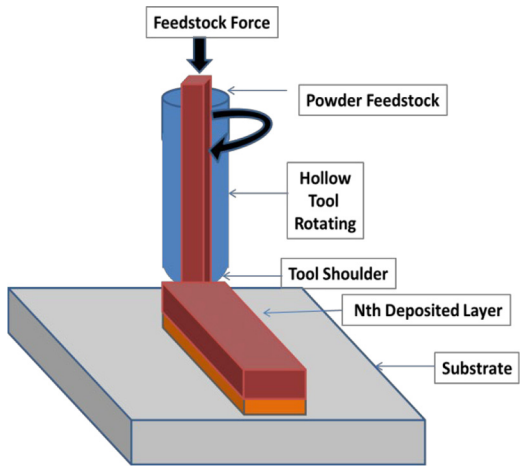

3.1.8 Laser cladding

Laser cladding shown in Figure 10 amongst other surface treatment techniques is one of the most operational methods attributed to its efficiency, flexibility and excellent metallurgical bonding between the substrate and the coating. Like laser surface alloying, the process involves the bonding of additional but dissimilar metals via powder or wire feedstock on the substrate using a laser beam to synthesize a near-net shape for the HEA coatings. It is accomplished by extruding two metals through a die and rolling the sheets of metal together at high pressure (Santo, 2008). The laser cladding process is used for other applications like fabrication and repairing of components, renewal of damaged parts and synthesis of dissimilar materials.

1.1 Characteristics of a laser-deposition process as follows:

- This process can be successfully carried out under atmospheric conditions.
- The process guarantees strong metallurgical bonding between the substrate and the fully dense coating.
- The speed used for processing the coatings is very high.
- There is no need for clamping the substrate.
- Near-net-shape components require little or no finishing.
- It builds up small heat-affected zones with little or no damage to the base material.
- The process can fabricate coatings using hard or soft materials, by the same laser beam, only by adjusting the processing parameters.

Figure 10 Schematic diagram of the laser cladding process (Frenk and Kurz, 1993)

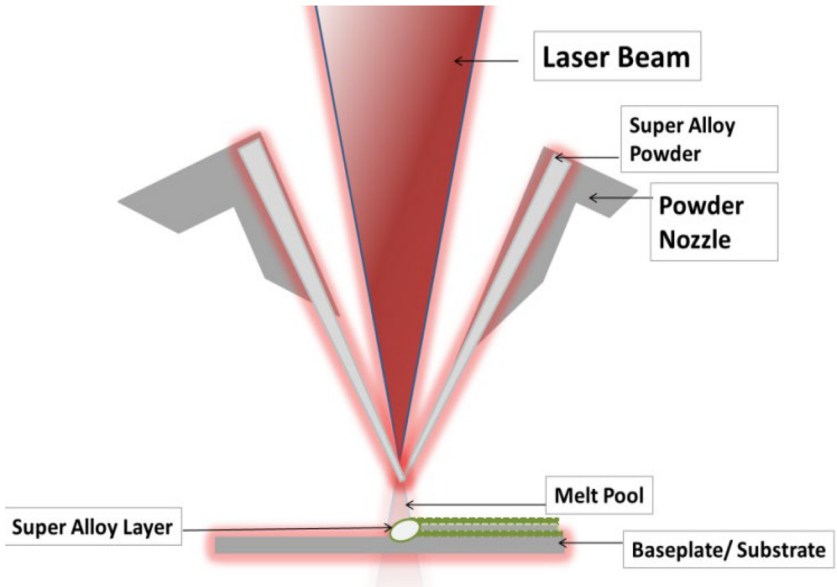

- Rapid cooling and solidification rates enhance the development of fine microstructures.
- There is a very low level of noise pollution and a high degree of flexibility of the user-friendly automated process.

3.2 Defects in the laser deposition technique process

The strength and quality of HEA components fabricated using lasers are mostly influenced by the physical behaviour of the material at the time of deposition (Fotovvati *et al.*, 2018). The solidification process, separation/segregation, development of the molten pool, the capillary effect, keyhole formation, amalgamation, the Marangoni effect, vapourization, entrapment of vapour and gas bubbles, spattering, shrinkage, phase transformations, explosion and instability of the molten pool, partial melting of powder particles and remelting processes are just a few of the physical behaviours' of the HEAs during fabrication that can lead to defects and imperfections (PalDrstvensek and Brajlih, 2018). These imperfections and defects can arise because of lack of fusion, porosity, spattering; cracks and when the laser processing parameters are not optimized (Tang and Pistorius, 2017). Inter-run and random porosity, which could be fine or coarse, are commonly formed in the laser cladding technique.

Cracking occurs as hot or cold cracks. A hot crack appears at high temperatures during solidification attributed to thermomechanical and metallurgical factors whilst cold cracks occur at lower temperatures. Furthermore, cold cracks are attributed to the presence of hydrogen in the heat-affected zone, martensitic formations and residual stresses (MarazaniMadyira and Akinlabi, 2017).

There are distinct types of spattering, namely; molten and/or powder particle spattering, which cause uneven distribution of the HEAs during deposition attributed to thermal shock, gas flow, the recoil pressure of the laser or metallic vapour. Spattering caused by explosion, vortex and keyhole effect is called a jet, big or small spattered particle (Anwar and Pham, 2017). Spattering occurs when inert gases in between the HEA powder particles get entrapped in the melt pool, which will eventually cause an explosion when the gas tries to expand (Ladewig *et al.*, 2016). The explosion, in turn, causes spattering. At high energy density and high scan speed, the chances of an explosion are higher, even so, at a low scan speed; the gas can easily expand without exploding. Still, lowering the scan speeds may cause unmelted zones. Therefore, spattering is mostly influenced by a high scan speed (Liu *et al.*, 2016).

The keyhole effect is a pore with a smooth surface wall and a corner point. This occurs when the bottom of a deposited HEA layer gets a higher temperature than the upper layer, which causes the bottom part to evaporate leaving a keyhole or void inside the melt pool (Fabbro, 2019). This can be resolved by increasing the energy density which releases surface tension and lowers the melt pool viscosity, thus preventing vapour entrapment and a keyhole effect. When excessive HEA powder is fed into the molten pool, there is a high probability of the powder particles to be un-melted (Dass and Moridi, 2019). This powder inefficiency in the melt pool is attributed to a low laser power at a very high speed. More so, improper melt pool formation which could be big or small, physically or thermally unstable, may happen due to a low energy density and a high scanning speed. A low energy density does not melt the powder particles and a high scanning speed provides rapid solidification, increasing the insufficiency of the time to melt these particles. Hence, the optimization of the process is necessary to avoid the keyhole effect (Andani *et al.*, 2018).

Gas entrapment occurs when gas bubbles which move with the vortex in the melt pool attributed to the thermal differences break into different pieces. After solidification, these entrapped bubbles become pores. High energy densities above the viscosity level of the melt pool can prevent the formation of pores by expelling gas bubbles through a resilience force by the liquid HEA.

Defects in the geometrical shape of the coating can arise because of the tilt in the laser's angle beam and surface waviness that occurs in the overlap ratio between clad tracks (Szemkus *et al.*, 2018). When the tracks are not properly overlapped, defects such as spattering, pores and bending will occur.

During shrinkage, the melt pool separates, forming micro-cracks and if the track overlap is low, these micro-cracks will remain becoming a defect. Shrinkage stresses during rapid cooling make the clad height susceptible to cracks when the contact angle between the substrate and the clad track becomes over 90° (Pal *et al.*, 2016).

Nonetheless, most defects associated with the laser cladding process can be eliminated by the optimization/regulation or control of the laser processing parameters and the use of heat treatments.

Other methods of surface modification include; organic coatings, diamond coating, electroforming, porcelain enamelling, Painting, water-jet peening, diffusion coating, hard facing, electroplating, conversion coating, shot peening, surface texturing, mechanical plating, hot dipping, explosive and case hardening (Agarwal and García, 2019; Ramappa and Jogikalmath, 2018).

3.3 Processing parameters

This includes the scanning speed, the beam focal point, the laser power and the beam diameter, to mention a few. These parameters influence the dilution rates, the clad geometry, the microstructure and properties of the coatings.

The laser power is the energy available to be absorbed by the molten pool, and this influences the surface morphology of the coatings. Optimization of the laser power is necessary because a high power can lead to crater formation and surface evaporation whilst a lower power can lead to inhomogeneous microstructures and inadequate mixing or bonding between the substrate and the HEA coating (Kaierle *et al.*, 2012). Optimal laser processing parameters of some laser-deposited HEAs systems are summarized in Table 2.

The beam focus position parameter is characterized by positive and negative defocus stages and a focus stage. In the negative defocus stage, there is an inadequate melting of the HEA powders and there is a high possibility of the powders rebounding from the surface without being deposited. In a positive defocused stage, the dilution and melted zone are too large, hence, abating the properties of the coating. On the other hand, a focus stage is optimal because The HEA powders are melted properly and there are no rebounds or large dilution or melted zones (Zhu *et al.*, 2012). The dilution rate is directly related to other parameters such as the scanning speed, laser power and focal position. It influences the HEA coatings thickness, the homogeneous microstructure and the bonding between the substrate and the coating (Huang, 2011). The scanning speed influences the heat and mass transfers, the molten pool and the cooling rates which also affect the composition and microstructure of the HEA coatings (Mugwagwa *et al.*, 2018). Powder feed rate is the velocity at which the powders are transferred by a non-reactive carrier gas through the powder feeding tubes to the molten pool. Increasing the feed rate increases the layer thickness of the HEA coatings and vice versa (Mrdak *et al.*, 2019).

3.4 Safety practices during fabrication

Different manufacturing processes have several dangers associated with human life and property. Industrial safety helps reduce accidents, deaths and component or equipment losses. Most hazards to humans associated with the fabrication processes are respiratory through the eyes, nose and skin. For laser processing, the contact of the laser and the eye could cause blindness, skin burns or skin cancers. Inhaling powder particles during fabrication could damage the lungs (Bours *et al.*, 2017). Standard safe practices are, therefore, necessary to prevent loss of life and damage to properties. These practices reduce hazards to the barest minimum and educate technicians on safety principles that increase productivity and enhance human relations (ChuaWong and Yeong, 2017). For these reasons, standard safety practices should be adhered to at all times, which include but not limited to; only trained authorized personnel should handle the equipment, personal protective gears should be worn at all times during fabrication, the fabrication equipment must be housed according to standard practices and safety programmes and/or training must be organized periodically (Seifi *et al.*, 2017).

3.5 Other surface modification techniques

The surface modification of components built by HEAs is a fundamental part of the alloy's functionality, it could be thermos-chemical, thermal or through coatings, however, these parts may become vulnerable to failure and deterioration due to tribological and mechanical challenges, as a result, determining the surface modification technique to apply involves the property that needs enhancements; fatigue, wear, creep strength, erosion and corrosion resistance (LiLiu and Liaw, 2018). Protective surfaces consist of scratch protection, diffusion barriers, friction reduction, local and transparent corrosion protection, accordingly, there are challenges faced without the improvements of the HEAs properties which can

Table 2 Optimal laser processing parameters of some laser-deposited HEAs system

HEA	Laser power (W)	Scan speed (mm/s)	Layer thickness (mm)	Overlap (%)	Phase	Ref
AlCoCrFeNi	600–800	8	0.25–0.7	50	BCC, B2	(Kunce *et al.*, 2015; Ocelík *et al.*, 2016; Wang *et al.*, 2017)
AlxCoCrFeNi	800–1,200	4–12	0.25	–	FCC, BCC, B2	(Chao *et al.*, 2017; Joseph *et al.*, 2015)
AlCoCrCuFe	1,000–3,000	4–20	–	30	FCC, BCC, L12, B2	(Li *et al.*, 2017)
AlCoCrCuFeNi	1,200–1,600	8–12	0.2	50	FCC, BCC	(Dada *et al.*, 2020)
AlCoCrCuFeNiTi	1,200–1,600	8–12	0.2	50	FCC, BCC, L12	(Dada *et al.*, 2020)

ultimately lead to limitations in its application and the failure of the advanced material during service (Mohit and Arul Mozhi Selvan, 2018).

Various processes of surface treatments of HEAs are applied based on chemical, thermal, mechanical and physical conditions which lead to the formation of homogeneous microstructures with excellent properties. Conventional Surface treatment methods include electroplating, cyaniding, anodizing, galvanizing, carbonitriding, Boronising, diffusion coating, nitriding, carburizing, thermal spraying and induction hardening (Mozetič, 2019). In recent times, other surface modification methods of HEAs have been adopted and some of these methods are discussed below.

3.5.1 Vapour deposition methods

There are several vapour deposition methods of HEAs and these techniques are shown in Figure 11 (Choy, 2003).

3.5.1.1 Physical vapour deposition. This can be defined as a vacuum deposition method (VDM) as shown in Figure 12. VDM produces thin films and coatings of metals, alloys and ceramics in thickness from 1 μm to 10 μm. There are different types of PVD, namely; sputtering, evaporation, molecular beam epitaxy and pulsed laser deposition (PLD) (Thijs *et al.*, 2010). Sputtering is the most widely used deposition method. The process parameters and the chemical composition of the target can be varied to control stoichiometry. Furthermore, the N_2, C_2H_2 reactive gas can be added during deposition, which gives the technique flexibility to explore a wide range of HEAF or coating systems.

Li *et al.* (2016) fabricated HEAs coating by magnetron sputtering and the authors reported that the coatings were perfectly dense and smooth with the FCC solid solution phase. The coatings were said to be more resistant to corrosion in both NaCl and H_2SO_4 solutions than the 201 stainless steel. Marshal *et al.* (2019) fabricated HEAs thin films using the same alloy as a target by direct current magnetron sputtering deposition process and the results also showed improvements in the properties of the alloys. Dang *et al.* (2018) used a high-vacuum radio frequency magnetron sputtering process to develop HEA thin films also using the films as the target and they stated that the films had the Nano-grain size of approximately 10 nm which can be applicable for micro-fabrication. On the other hand, Nagy *et al.* (2020) developed a novel multiple-beam sputtering that uses commercial pure metal targets instead of the conventional use of the HEAF targets. They argued that the novel method fabricated HEA thin films with excellent mechanical properties compared to conventional methods.

3.5.1.2 Chemical vapour deposition. Protective coatings are developed through chemical reactions between the HEAs' coating and the substrate in a gas precursor. It can either be an open reactor system or a closed reactor system (Pierson, 1999). The open reactor system consists of a thermal deposition which occurs at high temperatures whilst the plasma deposition or closed reactor occurs at lower temperatures on substrates with low melting points. Lal and Sundara (2019) investigated the use of high entropy oxide nanoparticles for the growth of carbon nanotube by chemical vapour deposition (CVD) and

Figure 11 Methods of vapour deposition

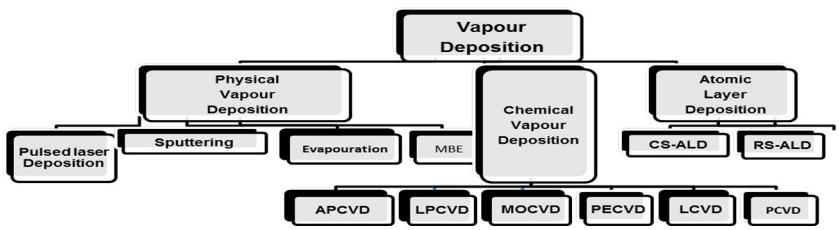

Figure 12 Schematic diagram of the PVD process (Mattox, 1998)

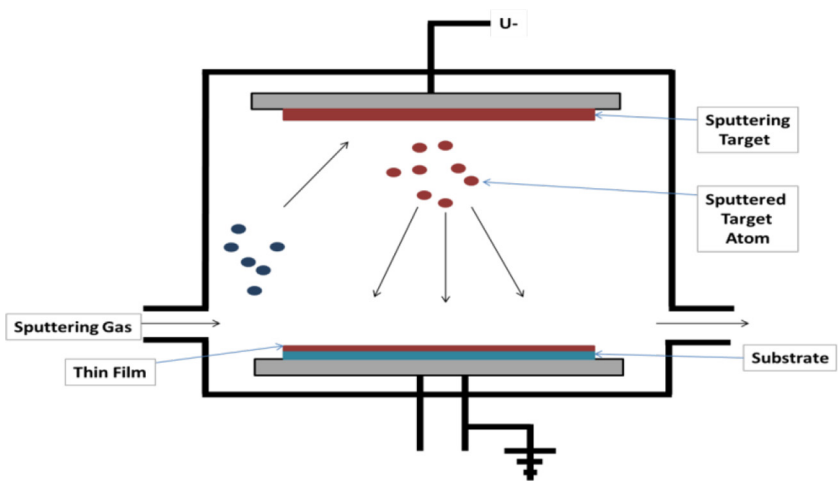

the study showed that the components fabricated had great potential for several energy applications. Nonetheless, the setback of CVD is the toxicity of the precursor chemicals and the build of the exhaust system in avoiding pollution (Zhang *et al.*, 2013).

3.5.1.3 Atomic layer deposition. This is defined as a deposition technique that uses a thin film established on a sequential gas-phase chemical process with two chemical precursors and these chemical precursors react with the surface of the HEA material sequentially. Through repetitive exposure separating the precursors, the thin film is then deposited. This fabrication technique is categorized into; chemisorption saturation-atomic layer deposition (ALD) process and sequential surface chemical reaction-ALD process (Bruck and Kamel, 2016).

These deposition processes are limited by their lack of flexibility, high consumption of energy, material wastage and poor precision alongside several environmental hazards.

The limitations of these aforementioned techniques make the LSM of HEAs which is characterized by coherence, homogeneous microstructure and excellent metallurgical bonding strength, reduction in grain growth and directionality, minimal dilution of the substrate, automation, cost-effectiveness, excellent quality and monochromaticity, a preferred manufacturing alternative. This technique allows an extensive range of surface treatments with only a small size laser beam as the only shortcoming; hence, laser surface treatments are considered the most effective method with application in re-manufacturing corroded, cracked or worn engineering parts (Mallick *et al.*, 2019).

4. Future recommendations

Structural components in the turbine engine need resistance against yielding or plastic deformation. Ductility and strength depend on the movement of dislocation and this dislocation may be hindered if there are discontinuities in its path, thus the need for precipitate strengthening. However, precipitates may cause decreased ductility and premature failure because they are hardening the material and may become obstacles to dislocation glide in the process. In most cases, it is difficult for a material to have both strength and ductility, however, densely dispersed nano precipitates is recommended as a proficient addition to providing a homogeneous and sustainable hardening deformation mechanism that enhances both strength and ductility in both HEAs and HESAs. This mechanism is governed by the gap between the matrix and the precipitate and can be fully used to develop an excellent combination of ductility and strength in alloys. Although the HESAs currently have more advantages over the Nickel-based superalloy, the size of the HESAs ordered γ'' particles, the optimum volume fraction and the γ'' solvus temperature still need to be improved and investigated. Process optimization of the fluence and pulse duration in the laser ablation fabrication of HEAs should be investigated. Limited studies in the literature can be found on the Laser ablation of high entropy nanoparticle decorated with graphene as the first report on the material was achieved through mechanical milling and sonication. *In situ* surface modification and fabrication is a process that has promising potential to be an alternative to existing or conventional methods; therefore, further studies should be done and reported. Furthermore, reports on the coating of HEAs with nano hierarchical structures are currently limited in the literature. Investigating this aspect of metallurgy may provide surface textures with anti-reflection, optical transparency and superhydrophobicity. Characterization of HEAs should be broadened to studying detailed mechanical attributes of the amalgams, such as fatigue, tensile, fracture and creep. The low ductility of BCC HEAs and the limitations of the FCC HEAs attributed to necking should be researched and improved. Despite identifying the laser friction stir deposition as a fourth industrial revolution process, other more economical and viable processes for deposition and joining of HEAs should be explored. Whilst the optimizations of laser parameters of the friction stir process, feedstock preparation and the adoption of the HEA material and coating in the industry should be of great interest alongside the investigation of dissimilar joints.

5. Conclusion

This study reviews the advances in HEA material and fabrication techniques. We have presented HESAs as an alternative to conventional superalloys currently used in the aerospace industry due to their exceptional properties; however, there are limited records on the industrial application of these superalloys. There are so many opportunities in material design using the high entropy effect, with the introduction of HEPs, ceramics, steels and films, to mention a few. The $Al_xCoCrCuFeNi$ HEA system, particularly the $Al_{0.5}CoCrCuFeNi$ HEA has been extensively studied, attributed to its mechanical and physical properties exceeding that of pure metals for aerospace turbine engine applications and the advances in the fabrication and surface modification processes of the alloy was outlined to show the latest developments focusing on laser-based manufacturing processing due to its many advantages. Laser AM techniques produce defect-free components once the process is optimized, as opposed to conventional techniques. Laser-based methods are ideal for surface modifications and protective treatments for HEAs as long as safety practices are observed during fabrication to avoid damage to lives and properties.

References

Agarwal, R. and García, A.J. (2019), "Surface modification of biomaterials", *Principles of Regenerative Medicine*, Elsevier, pp. 651-660.

Agrawal, P., Shukla, S., Gupta, S., Agrawal, P. and Mishra, R. S. (2020), "Friction stir gradient alloying: a high-throughput method to explore the influence of V in enabling HCP to BCC transformation in a γ-FCC dominated high entropy alloy", *Applied Materials Today*, Vol. 21 No. 100853.

Alemohammad, S.H. (2010), "Development of optical fiber-based sensing devices using laser microfabrication methods".

Alshataif, Y.A., Sivasankaran, S., Al-Mufadi, F.A., Alaboodi, A.S. and Ammar, H.R. (2019), "Manufacturing methods, microstructural and mechanical properties evolutions of high-entropy alloys: a review", *Metals and Materials International*, pp. 1-35.

Anand, G., Wynn, A.P., Handley, C.M. and Freeman, C.L. (2018), "Phase stability and distortion in high-entropy oxides", *Acta Materialia*, Vol. 146, pp. 119-125.

Andani, M.T., Dehghani, R., Karamooz-Ravari, M.R. Mirzaeifar, R. and NI., J. (2018), "A study on the effect of energy input on spatter particles creation during selective laser melting process", *Additive Manufacturing*, Vol. 20, pp. 33-43.

Antonialli, A.Í.S., Carvalho, M.R.D.D. and Diniz, A.E. (2020), "On the machinability of the Ni-30 high-temperature iron-based superalloy", *Journal of the Brazilian Society of Mechanical Sciences and Engineering*, Vol. 42 No. 10, pp. 1-11.

Anwar, A.B. and Pham, Q.C. (2017), "Selective laser melting of AlSi10Mg: effects of scan direction, part placement and inert gas flow velocity on tensile strength", *Journal of Materials Processing Technology*, Vol. 240, pp. 388-396.

Ashby, M. and Greer, A.L. (2006), "Metallic glasses as structural materials", *Scripta Materialia*, Vol. 54 No. 3, pp. 321-326.

Atkins, P. (2010), *The Laws of Thermodynamics: A Very Short Introduction*, OUP Oxford.

Baburaj, E., Starikov, D., Evans, J., Shafeev, G. and Bensaoula, A. (2007), "Enhancement of adhesive joint strength by laser surface modification", *International Journal of Adhesion and Adhesives*, Vol. 27 No. 4, pp. 268-276.

Baker, I. (2020), "Interstitials in fcc high entropy alloys", *Metals*, Vol. 10 No. 5, p. 695.

Ball, P. (1999), "Engineering shark skin and other solutions", *Nature*, Vol. 400 No. 6744, pp. 507-509.

Bera, M.N., Riera, A., Lewenstein, M. and Winter, A. (2016), "Universal laws of thermodynamics", at https://arxiv.org/abs/1612.04779

Bérardan, D., Franger, S., Dragoe, D., Meena, A.K. and Dragoe, N. (2016), "Colossal dielectric constant in high entropy oxides", *Physica Status Solidi (Rrl) – Rapid Research Letters*, Vol. 10 No. 4, pp. 328-333.

Berardan, D., Meena, A., Franger, S., Herrero, C. and Dragoe, N. (2017), "Controlled Jahn-Teller distortion in (MgCoNiCuZn) O-based high entropy oxides", *Journal of Alloys and Compounds*, Vol. 704, pp. 693-700.

Best, J.P., Ostergaard, H.E., Li, B., Stolpe, M., Yang, F., Nomoto, K., Hasib, M.T., Muránsky, O., Busch, R. and Li, X. (2020), "Fracture and fatigue behaviour of a laser additive manufactured Zr-based bulk metallic glass", *Additive Manufacturing*, Vol. 36, p. 101416.

Bianchi, V., Carey, T., Viti, L., LI., L., Linfield, E.H., Davies, A.G., Tredicucci, A., Yoon, D., Karagiannidis, P.G. and Lombardi, L. (2017), "Terahertz saturable absorbers from liquid phase exfoliation of graphite", *Nature Communications*, Vol. 8 No. 1, pp. 1-9.

Birosca, S., Liu, G., Ding, R., Jiang, J., Simm, T., Deen, C. and Whittaker, M. (2019), "The dislocation behaviour and GND development in a nickel based superalloy during creep", *International Journal of Plasticity*, Vol. 118, pp. 252-268.

Bocchini, P.J., Sudbrack, C.K., Noebe, R.D., Dunand, D.C. and Seidman, D.N. (2017), "Microstructural and creep properties of boron-and zirconium-containing cobalt-based superalloys", *Materials Science and Engineering: A*, Vol. 682, pp. 260-269.

Bours, J., Adzima, B., Gladwin, S., Cabral, J. and Mau, S. (2017), "Addressing hazardous implications of additive manufacturing: complementing life cycle assessment with a framework for evaluating direct human health and environmental impacts", *Journal of Industrial Ecology*, Vol. 21 No. S1, pp. S25-S36.

Boyer, R.R. (1996), "An overview on the use of titanium in the aerospace industry", *Materials Science and Engineering: A*, Vol. 213 Nos 1/2, pp. 103-114.

Braic, V., Balaceanu, M., Braic, M., Vladescu, A., Panseri, S. and Russo, A. (2012a), "Characterization of multi-principal-element (TiZrNbHfTa) N and (TiZrNbHfTa) C coatings for biomedical applications", *Journal of the Mechanical Behavior of Biomedical Materials*, Vol. 10, pp. 197-205.

Braic, V., Vladescu, A., Balaceanu, M., Luculescu, C. and Braic, M. (2012b), "Nanostructured multi-element (TiZrNbHfTa) N and (TiZrNbHfTa) C hard coatings", *Surface and Coatings Technology*, Vol. 211, pp. 117-121.

Brandao, F., Horodecki, M., N.G., N., Oppenheim, J. and Wehner, S. (2015), "The second laws of quantum thermodynamics", *Proceedings of the National Academy of Sciences*, Vol. 112 No. 11, pp. 3275-3279.

Brechtl, J., Chen, S., Xie, X., Ren, Y., Qiao, J., Liaw, P. and Zinkle, S. (2019), "Towards a greater understanding of serrated flows in an Al-containing high-entropy-based alloy", *International Journal of Plasticity*, Vol. 115, pp. 71-92.

Brif, Y., Thomas, M. and Todd, I. (2015), "The use of high-entropy alloys in additive manufacturing", *Scripta Materialia*, Vol. 99, pp. 93-96.

Brown, T.L., Lemay, H.E., JR,. and Bursten, B.E. (2005), *Chemical thermodynamics. Chemical Thermodynamics of Zirconium*, NEA OECD, Elsevier, ISBN-13:978-970.

Bruck, G.J. and Kamel, A. (2016), "Deposition of superalloys using powdered flux and metal. Google patents".

Cabibbo, M., Gariboldi, E., Spigarelli, S. and Ripamonti, D. (2008), "Creep behavior of INCOLOY alloy 617", *Journal of Materials Science*, Vol. 43 No. 8, pp. 2912-2921.

Cantor, B., Chang, I., Knight, P. and Vincent, A. (2004), "Microstructural development in equiatomic multicomponent alloys", *Materials Science and Engineering: A*, Vol. 375, pp. 213-218.

Cao, D., Wu, Y., L.I., H., Liu, X., Wang, H., Wang, X. and Lu, Z. (2018), "Beneficial effects of oxygen addition on glass formation in a high-entropy bulk metallic glass", *Intermetallics*, Vol. 99, pp. 44-50.

Chang, S.Y., Chen, M.K. and Chen, D.S. (2009), "Multiprincipal-element AlCrTaTiZr-nitride nanocomposite film of extremely high thermal stability as diffusion barrier for Cu metallization", *Journal of the Electrochemical Society*, Vol. 156 No. 5, p. G37.

Chang, R., Fang, W., Yu, H., Bai, X., Zhang, X., Liu, B. and Yin, F. (2019), "Heterogeneous banded precipitation of (CoCrNi) 93Mo7 medium entropy alloys towards strength–ductility synergy utilizing compositional inhomogeneity", *Scripta Materialia*, Vol. 172, pp. 144-148.

Chang, S.Y., Huang, Y.C., L.I., C.E., Hsu, H.F., Yeh, J.W. and Lin, S.J. (2013), "Improved diffusion-resistant ability of multicomponent nitrides: from unitary TiN to senary high-

entropy (TiTaCrZrAlRu) N", *JOM*, Vol. 65 No. 12, pp. 1790-1796.

Chao, Q., Guo, T., Jarvis, T., Wu, X., Hodgson, P. and Fabijanic, D. (2017), "Direct laser deposition cladding of AlxCoCrFeNi high entropy alloys on a high-temperature stainless steel", *Surface and Coatings Technology*, Vol. 332, pp. 440-451.

Chatterjee, P., Athawale, V.M. and Chakraborty, S. (2009), "Selection of materials using compromise ranking and outranking methods", *Materials & Design*, Vol. 30 No. 10, pp. 4043-4053.

Chatterjee, A. and Deopura, B. (2002), "Carbon nanotubes and nanofibre: an overview", *Fibers and Polymers*, Vol. 3 No. 4, pp. 134-139.

Chawla, V., Prakash, S., Puri, D. and Singh, B. (2009), "Corrosion behavior of nanostructured TiAlN and AlCrN hard coatings on superfer 800H superalloy in simulated marine environment", *Journal of Minerals and Materials Characterization and Engineering*, Vol. 08 No. 09, pp. 693-700.

Chen, Y.T., Chang, Y.J., Murakami, H., Sasaki, T., Hono, K., Li, C.W., Kakehi, K., Yeh, J.W. and Yeh, A.C. (2020), "Hierarchical microstructure strengthening in a single crystal high entropy superalloy", *Scientific Reports*, Vol. 10 No. 1, pp. 1-11.

Cheng, H., Liu, X., Tang, Q., Wang, W., Yan, X. and Dai, P. (2019), "Microstructure and mechanical properties of FeCoCrNiMnAlx high-entropy alloys prepared by mechanical alloying and hot-pressed sintering", *Journal of Alloys and Compounds*, Vol. 775, pp. 742-751.

Cheng, J., Sun, B., Ge, Y., Hu, X., Zhang, L., Liang, X. and Zhang, X. (2020), "Nb doping in laser-cladded Fe25Co25Ni25 (B0. 7Si0. 3) 25 high entropy alloy coatings: microstructure evolution and wear behavior", *Surface and Coatings Technology*, Vol. 402, p. 126321.

Chen, M.R., Lin, S.J., Yeh, J.W., Chuang, M.H., Chen, S.K. and Huang, Y.S. (2006), "Effect of vanadium addition on the microstructure, hardness, and wear resistance of Al 0.5 CoCrCuFeNi high-entropy alloy", *Metallurgical and Materials Transactions A*, Vol. 37 No. 5, pp. 1363-1369.

Chen, H., Lin, W., Zhang, Z., Jie, K., Mullins, D.R., Sang, X., Yang, S.Z., Jafta, C.J., Bridges, C.A. and Hu, X. (2019), "Mechanochemical synthesis of high entropy oxide materials under ambient conditions: dispersion of catalysts via entropy maximization", *ACS Materials Letters*, Vol. 1 No. 1, pp. 83-88.

Chen, T., Shun, T., Yeh, J. and Wong, M. (2004), "Nanostructured nitride films of multi-element high-entropy alloys by reactive DC sputtering", *Surface and Coatings Technology*, Vol. 188, pp. 193-200.

Chen, T.K. and Wong, M.S. (2008), "Hard transparent conducting hex-element complex oxide films by reactive sputtering", *Journal of Materials Research*, Vol. 23 No. 11, pp. 3075-3089.

Chen, T.K., Wong, M.S., Shun, T.T. and Yeh, J.W. (2005), "Nanostructured nitride films of multi-element high-entropy alloys by reactive DC sputtering", *Surface and Coatings Technology*, Vol. 200 Nos 5/6, pp. 1361-1365.

Chen, C.S., Yang, C.C., Chai, H.Y., Yeh, J.W. and Chau, J.L. H. (2014), "Novel cermet material of WC/multi-element alloy", *International Journal of Refractory Metals and Hard Materials*, Vol. 43, pp. 200-204.

Chen, H., Fu, J., Zhang, P., Peng, H., Abney, C.W., Jie, K., Liu, X., Chi, M. and Dai, S. (2018a), "Entropy-stabilized metal oxide solid solutions as CO oxidation catalysts with high-temperature stability", *Journal of Materials Chemistry A*, Vol. 6 No. 24, pp. 11129-11133.

Chen, J., Yao, Z., Wang, X., Lu, Y., Wang, X., Liu, Y. and Fan, X. (2018b), "Effect of C content on microstructure and tensile properties of as-cast CoCrFeMnNi high entropy alloy", *Materials Chemistry and Physics*, Vol. 210, pp. 136-145.

Chen, J., Zhou, X., Wang, W., Liu, B., Lv, Y., Yang, W., Xu, D. and Liu, Y. (2018c), "A review on fundamental of high entropy alloys with promising high–temperature properties", *Journal of Alloys and Compounds*, Vol. 760, pp. 15-30.

Chen, K., Pei, X., Tang, L., Cheng, H., Li, Z., L.I., C., Zhang, X. and An, L. (2018d), "A five-component entropy-stabilized fluorite oxide", *Journal of the European Ceramic Society*, Vol. 38 No. 11, pp. 4161-4164.

Choy, K. (2003), "Chemical vapour deposition of coatings", *Progress in Materials Science*, Vol. 48 No. 2, pp. 57-170.

Chua, C.K., Wong, C.H. and Yeong, W.Y. (2017), *Standards, Quality Control, and Measurement Sciences in 3D Printing and Additive Manufacturing*, Academic Press.

Chung, D.W., Toinin, J.P., Lass, E.A., Seidman, D.N. and Dunand, D.C. (2020a), "Effects of Cr on the properties of multicomponent cobalt-based superalloys with ultra high γ'volume fraction", *Journal of Alloys and Compounds*, Vol. 832, p. 154790.

Chung, D.W., Toinin, J.P., Lass, E.A., Seidman, D.N. and Dunand, D.C. (2020b), "Effects of Cr on the properties of multicomponent cobalt-based superalloys with ultra high γ'volume fraction", *Journal of Alloys and Compounds*, Vol. 832 No. 154790.

Clauer, A.H. (1996), "Laser shock peening for fatigue resistance", *Surface Performance of Titanium*, Vol. 217, p. 230.

Clemens, H. and Smarsly, W. (2011), "Light-weight intermetallic titanium aluminides–status of research and development", *Advanced Materials Research*, Vol. 278, pp. 551-556.

Contin, A., Alves, K.A., Campos, R.A., Vasconcelos, G.D., Damm, D.D., Trava-Airoldi, V.J. and Corat, E.J. (2017), "Diamond films on stainless steel substrates with an interlayer applied by laser cladding", *Materials Research*, Vol. 20 No. 2, pp. 543-548.

Cui, P., Li, W., Liu, P., Zhang, K., Ma, F., Chen, X., Feng, R. and Liaw, P.K. (2020), "Effects of nitrogen content on microstructures and mechanical properties of (AlCrTiZrHf) N high-entropy alloy nitride films", *Journal of Alloys and Compounds*, Vol. 834 No. 155063.

Dada, M., Popoola, P., Mathe, N., Adeosun, S., Pityana, S., Aramide, O., Malatji, N., Lengopeng, T. and Ayodeji, A. (2021), "Recent advances of high entropy alloys: high entropy superalloys", *Advances in High-Entropy Alloys-Materials Research, Exotic Properties and Applications*.

Dada, M., Popoola, P., Mathe, N., Pityana, S., Adeosun, S., Aramide, O. and Lengopeng, T. (2020), "Process

optimization of high entropy alloys by laser additive manufacturing", *Engineering Reports*, Vol. 2 No. 10.

Dang, C., Surjadi, J.U., Gao, L. and Lu, Y. (2018), "Mechanical properties of nanostructured CoCrFeNiMn high-entropy alloy (HEA) coating", *Frontiers in Materials*, Vol. 5, p. 41.

Dass, A. and Moridi, A. (2019), "State of the art in directed energy deposition: from additive manufacturing to materials design", *Coatings*, Vol. 9 No. 7, p. 418.

DE Cicco, H., Luppo, M., Gribaudo, L. and Ovejero-GARCıA, J. (2004), "Microstructural development and creep behavior in A286 superalloy", *Materials Characterization*, Vol. 52 No. 2, pp. 85-92.

Diercks, D.R., Brennecka, G., Gorman, B.P., Rost, C.M. and Maria, J.P. (2017), "Nanoscale compositional analysis of a thermally processed entropy-stabilized oxide via correlative TEM and APT", *Microscopy and Microanalysis*, Vol. 23 No. S1, pp. 1640-1641.

Ding, Q., L.I., S., Chen, L.Q., Han, X., Zhang, Z., Yu, Q. and Li, J. (2018), "Re segregation at interfacial dislocation network in a nickel-based superalloy", *Acta Materialia*, Vol. 154, pp. 137-146.

Ding, K. and Ye, L. (2006), *Laser Shock Peening: performance and Process Simulation*, Woodhead Publishing.

Ding, Q., Zhang, Y., Chen, X., Fu, X., Chen, D., Chen, S., Gu, L., Wei, F., Bei, H. and Gao, Y. (2019), "Tuning element distribution, structure and properties by composition in high-entropy alloys", *Nature*, Vol. 574 No. 7777, pp. 223-227.

Dolique, V., Thomann, A.L., Brault, P., Tessier, Y. and Gillon, P. (2009), "Complex structure/composition relationship in thin films of AlCoCrCuFeNi high entropy alloy", *Materials Chemistry and Physics*, Vol. 117 No. 1, pp. 142-147.

Dong, L., King, W.P., Raleigh, M. and Wadley, H.N. (2018), "A microfabrication approach for making metallic mechanical metamaterials", *Materials & Design*, Vol. 160, pp. 147-168.

Eißmann, N., Klöden, B., Weißgärber, T. and Kieback, B. (2017), "High-entropy alloy CoCrFeMnNi produced by powder metallurgy", *Powder Metallurgy*, Vol. 60 No. 3, pp. 184-197.

EL-Bashir, S., Alsalhi, M., Al-Faifi, F. and Alenazi, W. (2019), "Spectral properties of PMMA films doped by perylene dyestuffs for photoselective greenhouse cladding applications", *Polymers*, Vol. 11 No. 3, p. 494.

Emmelmann, C., Kranz, J., Herzog, D. and Wycisk, E. (2013), "Laser additive manufacturing of metals", *Laser technology in biomimetics*. Springer, pp. 143-162.

Etsion, I. (2005), "State of the art in laser surface texturing", *Journal of Tribology*, Vol. 127 No. 1, pp. 248-253.

Fabbro, R. (2019), "Scaling laws for the laser welding process in keyhole mode", *Journal of Materials Processing Technology*, Vol. 264, pp. 346-351.

Fang, S., Wang, C., Li, C.L., Luan, J.H., Jiao, Z.B., Liu, C.T. and Hsueh, C.H. (2020), "Microstructures and mechanical properties of CoCrFeMnNiVx high entropy alloy films", *Journal of Alloys and Compounds*, Vol. 820 No. 153388.

Farotade, G.A. and Popoola, A.P. (2017), "A study on microhardness and microstructural evolution of titanium/zirconium diboride cermet coatings with varying scan speeds during laser cladding on Ti6Al4V substrate", *International Journal of Microstructure and Materials Properties*, Vol. 12 Nos 1/2, pp. 25-37.

Fisher, D. (2015), "High-Entropy Alloys-Microstructures and properties", *Foundations of Materials Science and Engineering*, Vol. 86, p. I.

Fotovvati, B., Wayne, S.F., Lewis, G. and Asadi, E. (2018), "A review on melt-Pool characteristics in laser welding of metals", *Advances in Materials Science and Engineering*, Vol. 2018.

Frazier, W.E. (2014), "Metal additive manufacturing: a review", *Journal of Materials Engineering and Performance*, Vol. 23 No. 6, pp. 1917-1928.

Frenk, A. and Kurz, W. (1993), "High speed laser cladding: solidification conditions and microstructure of a cobalt-based alloy", *Materials Science and Engineering: A*, Vol. 173 Nos 1/2, pp. 339-342.

Fu, Z., Chen, W., Xiao, H., Zhou, L., Zhu, D. and Yang, S. (2013), "Fabrication and properties of nanocrystalline Co0. 5FeNiCrTi0. 5 high entropy alloy by MA–SPS technique", *Materials & Design*, Vol. 44, pp. 535-539.

Gao, M.C. and Alman, D.E. (2013), "Searching for next single-phase high-entropy alloy compositions", *Entropy*, Vol. 15 No. 12, pp. 4504-4519.

Gao, M., Carney, C., Doğan, Ö., Jablonksi, P., Hawk, J. and Alman, D. (2015), "Design of refractory high-entropy alloys", *JOM*, Vol. 67 No. 11, pp. 2653-2669.

Gao, X., Zhao, K., Ke, H., Ding, D., Wang, W. and Bai, H. (2011), "High mixing entropy bulk metallic glasses", *Journal of Non-Crystalline Solids*, Vol. 357 No. 21, pp. 3557-3560.

Gattass, R.R. and Mazur, E. (2008), "Femtosecond laser micromachining in transparent materials", *Nature Photonics*, Vol. 2 No. 4, pp. 219-225.

Gebhardt, A. (2011), *Understanding additive manufacturing*.

Gild, J., Braun, J., Kaufmann, K., Marin, E., Harrington, T., Hopkins, P., Vecchio, K. and Luo, J. (2019), "A high-entropy silicide:(Mo0. 2Nb0. 2Ta0. 2Ti0. 2W0. 2) Si2", *Journal of Materiomics*, Vol. 5 No. 3, pp. 337-343.

Gild, J., Samiee, M., Braun, J.L., Harrington, T., Vega, H., Hopkins, P.E., Vecchio, K. and Luo, J. (2018), "High-entropy fluorite oxides", *Journal of the European Ceramic Society*, Vol. 38 No. 10, pp. 3578-3584.

Gild, J., Zhang, Y., Harrington, T., Jiang, S., Hu, T., Quinn, M.C., Mellor, W.M., Zhou, N., Vecchio, K. and Luo, J. (2016), "High-entropy metal diborides: a new class of high-entropy materials and a new type of ultrahigh temperature ceramics", *Scientific Reports*, Vol. 6 No. 1, pp. 1-10.

Gludovatz, B., Hohenwarter, A., Catoor, D., Chang, E.H., George, E.P. and Ritchie, R.O. (2014), "A fracture-resistant high-entropy alloy for cryogenic applications", *Science*, Vol. 345 No. 6201, pp. 1153-1158.

Gopan, V., Wins, K.L.D. and Surendran, A. (2021), "Innovative potential of additive friction stir deposition among current laser based metal additive manufacturing processes: a review", *CIRP Journal of Manufacturing Science and Technology*, Vol. 32, pp. 228-248.

Gorsse, S., Chen, Y.T., Hsu, W.C., Murakami, H. and Yeh, A.C. (2021), "Modeling the precipitation processes and the formation of hierarchical microstructures in a single crystal

high entropy superalloy", *Scripta Materialia*, Vol. 193, pp. 147-152.

Gorsse, S., Couzinié, J.P. and Miracle, D.B. (2018), "From high-entropy alloys to complex concentrated alloys", *Comptes Rendus Physique*, Vol. 19 No. 8, pp. 721-736.

Guo, L., GU., J., Gong, X., LI., K., NI., S., Liu, Y. and Song, M. (2019), "Short-range ordering induced serrated flow in a carbon contained", *FeCoCrNiMn High Entropy Alloy. Micron*, Vol. 126 No. 102739.

Guo, S., Ng, C., Lu, J. and Liu, C. (2011), "Effect of valence electron concentration on stability of fcc or bcc phase in high entropy alloys", *Journal of Applied Physics*, Vol. 109 No. 10, p. 103505.

Gupta, M.K., Mia, M., Pruncu, C.I., Kapłonek, W., Nadolny, K., Patra, K., Mikolajczyk, T., Pimenov, D.Y., Sarikaya, M. and Sharma, V.S. (2019), "Parametric optimization and process capability analysis for machining of nickel-based superalloy", *The International Journal of Advanced Manufacturing Technology*, Vol. 102 Nos 9/12, pp. 3995-4009.

Gwalani, B. (2017), *Developing Precipitation Hardenable High Entropy Alloys*, PhDT.

Haase, C., Tang, F., Wilms, M.B., Weisheit, A. and Hallstedt, B. (2017), "Combining thermodynamic modeling and 3D printing of elemental powder blends for high-throughput investigation of high-entropy alloys–towards rapid alloy screening and design", *Materials Science and Engineering: A*, Vol. 688, pp. 180-189.

Haratian, S. (2020), "Surface engineering of ZrCuAl-based bulk metallic glasses by gaseous oxidizing".

Heavens, O. (1950), "Some factors influencing the adhesion of films produced by vacuum evaporation", *Journal de Physique et le Radium*, Vol. 11 No. 7, pp. 355-360.

He, J., Liu, W., Wang, H., Wu, Y., L.I.U., X. and Nieh, T., & L.U., Z. (2014), "Effects of Al addition on structural evolution and tensile properties of the FeCoNiCrMn high-entropy alloy system", *Acta Materialia*, Vol. 62, pp. 105-113.

Hemphill, E.A. (2012), "Fatigue behavior of Al0. 5CoCrCuFeNi high entropy alloys", *Acta Materialia*, Vol. 60 No. 16, pp. 5723-5734.

Hemphill, M.A., Yuan, T., Wang, G., Yeh, J., Tsai, C., Chuang, A. and Liaw, P. (2012), "Fatigue behavior of Al0. 5CoCrCuFeNi high entropy alloys", *Acta Materialia*, Vol. 60 No. 16, pp. 5723-5734.

Herzog, D., Seyda, V., Wycisk, E. and Emmelmann, C. (2016), "Additive manufacturing of metals", *Acta Materialia*, Vol. 117, pp. 371-392.

He, J., Wang, H., Huang, H., Xu, X., Chen, M., Wu, Y., Liu, X., Nieh, T., A.N., K. and Lu, Z. (2016), "A precipitation-hardened high-entropy alloy with outstanding tensile properties", *Acta Materialia*, Vol. 102, pp. 187-196.

Hsu, Y.C., Li, C.L. and Hsueh, C.H. (2020), "Effects of Al addition on microstructures and mechanical properties of CoCrFeMnNiAlx high entropy alloy films", *Entropy*, Vol. 22 No. 1, p. 2.

Huang, Y. (2011), "Characterization of dilution action in laser-induction hybrid cladding", *Optics & Laser Technology*, Vol. 43 No. 5, pp. 965-973.

Huang, K., Chen, L., Lin, X., Huang, H., Tang, S. and Du, F. (2018), "Wear and corrosion resistance of Al0. 5CoCrCuFeNi high-entropy alloy coating deposited on AZ91D magnesium alloy by laser cladding", *Entropy*, Vol. 20 No. 12, p. 915.

Huang, Y.S., Chen, L., Lui, H.W., Cai, M.H. and Yeh, J.W. (2007), "Microstructure, hardness, resistivity and thermal stability of sputtered oxide films of AlCoCrCu0. 5NiFe high-entropy alloy", *Materials Science and Engineering: A*, Vol. 457 Nos 1/2, pp. 77-83.

Huang, Y.J., Yeh, J.W. and Yang, A.C.M. (2021), "High-entropy polymers': a new route of polymer mixing with suppressed phase separation", *Materialia*, Vol. 15 No. 100978.

Huang, C., Zhang, Y., Vilar, R. and Shen, J. (2012), "Dry sliding wear behavior of laser clad TiVCrAlSi high entropy alloy coatings on Ti–6Al–4V substrate", *Materials & Design*, Vol. 41, pp. 338-343.

Hummel, R.E. (2004), *Understanding Materials Science: history, Properties, Applications*, Springer Science & Business Media.

Ikeda, Y., Grabowski, B. and Körmann, F. (2019), "Ab initio phase stabilities and mechanical properties of multicomponent alloys: a comprehensive review for high entropy alloys and compositionally complex alloys", *Materials Characterization*, Vol. 147, pp. 464-511.

Ikeda, T. and Satoh, H. (1991), "Phase formation and characterization of hard coatings in the Ti–Al– N system prepared by the cathodic arc ion plating method", *Thin Solid Films*, Vol. 195 No. 1-2, pp. 99-110.

Jablonski, P.D., Licavoli, J.J., Gao, M.C. and Hawk, J.A. (2015), "Manufacturing of high entropy alloys", *JOM*, Vol. 67 No. 10, pp. 2278-2287.

Jain, H., Shadangi, Y., Shivam, V., Chakravarty, D., Mukhopadhyay, N. and Kumar, D. (2020), "Phase evolution and mechanical properties of non-equiatomic Fe–Mn–Ni–Cr–Al–Si–C high entropy steel", *Journal of Alloys and Compounds*, Vol. 834 No. 155013.

Jensen, J., Welk, B., Williams, R., Sosa, J., Huber, D., Senkov, O., Viswanathan, G. and Fraser, H. (2016), "Characterization of the microstructure of the compositionally complex alloy Al1Mo0. 5Nb1Ta0. 5Ti1Zr1", *Scripta Materialia*, Vol. 121, pp. 1-4.

Jiang, C., L.I., R., Wang, X., Shang, H., Zhang, Y. and Liaw, P.K. (2020), "Diffusion barrier performance of AlCrTaTiZr/AlCrTaTiZr-N high-entropy alloy films for Cu/Si connect system", *Entropy*, Vol. 22 No. 2, p. 234.

Jien-Wei, Y. (2006), "Recent progress in high entropy alloys", *Ann. Chim. Sci. Mat*, Vol. 31 No. 6, pp. 633-648.

Jin, T., Sang, X., Unocic, R.R., Kinch, R.T., Liu, X., Hu, J., Liu, H. and Dai, S. (2018), "Mechanochemical-assisted synthesis of high-entropy metal nitride via a soft urea strategy", *Advanced Materials*, Vol. 30 No. 23, p. 1707512.

Jokisaari, A.M., Naghavi, S.S., Wolverton, C., Voorhees, P.W. and Heinonen, O.G. (2017), "Predicting the morphologies of γ precipitates in cobalt-based superalloys", *Acta Materialia*, Vol. 141, pp. 273-284.

Joseph, J. (2016), *Study of Direct Laser Fabricated High Entropy Alloys*, Deakin University.

Joseph, J., Jarvis, T., Wu, X., Stanford, N., Hodgson, P. and Fabijanic, D.M. (2015), "Comparative study of the microstructures and mechanical properties of direct laser fabricated and arc-melted AlxCoCrFeNi high entropy

alloys", *Materials Science and Engineering: A*, Vol. 633, pp. 184-193.

Juan, C.C., Tsai, M.H., Tsai, C.W., Lin, C.M., Wang, W.R., Yang, C.C., Chen, S.K., Lin, S.J. and Yeh, J.W. (2015), "Enhanced mechanical properties of HfMoTaTiZr and HfMoNbTaTiZr refractory high-entropy alloys", *Intermetallics*, Vol. 62, pp. 76-83.

Kaierle, S., Barroi, A., Noelke, C., Hermsdorf, J., Overmeyer, L. and Haferkamp, H. (2012), "Review on laser deposition welding: from micro to macro", *Physics Procedia*, Vol. 39, pp. 336-345.

Khan, N.A., Akhavan, B., Zhou, C., Zhou, H., Chang, L., Wang, Y., L.I.U., Y., Fu, L., Bilek, M.M. and Liu, Z. (2020), "RF magnetron sputtered AlCoCrCu0. 5FeNi high entropy alloy (HEA) thin films with tuned microstructure and chemical composition", *Journal of Alloys and Compounds*, Vol. 836 No. 155348.

Kim, K. and Kim, T. (2019), "Nanofabrication by thermal plasma jets: from nanoparticles to low-dimensional nanomaterials", *Journal of Applied Physics*, Vol. 125 No. 7, p. 070901.

King, D., Middleburgh, S., Mcgregor, A. and Cortie, M. (2016), "Predicting the formation and stability of single phase high-entropy alloys", *Acta Materialia*, Vol. 104, pp. 172-179.

Klement, W., Willens, R. and Duwez, P. (1960), "Non-crystalline structure in solidified gold–silicon alloys", *Nature*, Vol. 187 No. 4740, pp. 869-870.

Klenk, R., Walter, T., Schock, H.W. and Cahen, D. (1993), "A model for the successful growth of polycrystalline films of CuInSe2 by multisource physical vacuum evaporation", *Advanced Materials*, Vol. 5 No. 2, pp. 114-119.

Kobayashi, Y. and Shirai, K. (2008), "Multi-axis milling for micro-texturing", *International Journal of Precision Engineering and Manufacturing*, Vol. 9 No. 1, pp. 34-38.

Koch, C.C. (2017), "Nanocrystalline high-entropy alloys", *Journal of Materials Research*, Vol. 32 No. 18, pp. 3435-3444.

Kong, T., Kang, B., Ryu, H.J. and Hong, S.H. (2020), "Microstructures and enhanced mechanical properties of an oxide dispersion-strengthened Ni-rich high entropy superalloy fabricated by a powder metallurgical process", *Journal of Alloys and Compounds*, Vol. 839 No. 155724.

Krasnov, M. (1973), "Laseropuncture of anterior chamber angle in glaucoma", *American Journal of Ophthalmology*, Vol. 75 No. 4, pp. 674-678.

Krol, T., Baither, D. and Nembach, E. (2004), "The formation of precipitate free zones along grain boundaries in a superalloy and the ensuing effects on its plastic deformation", *Acta Materialia*, Vol. 52 No. 7, pp. 2095-2108.

Kuehl, R.O. and Kuehl, R. (2000), "Design of experiments: statistical principles of research design and analysis".

Kumar, G., Desai, A. and Schroers, J. (2011), "Bulk metallic glass: the smaller the better", *Advanced Materials*, Vol. 23 No. 4, pp. 461-476.

Kumar, R.R., Karunagaran, B., Kumar, V.S., Jeyachandran, Y., Mangalaraj, D. and Narayandass, S.K. (2003), "Structural properties of V2O5 thin films prepared by vacuum evaporation", *Materials Science in Semiconductor Processing*, Vol. 6 Nos 5/6, pp. 543-546.

Kumar, N., Tiwary, C.S. and Biswas, K. (2018), "Preparation of nanocrystalline high-entropy alloys via cryomilling of cast ingots", *Journal of Materials Science*, Vol. 53 No. 19, pp. 13411-13423.

Kunce, I., Polanski, M., Karczewski, K., Plocinski, T. and Kurzydlowski, K. (2015), "Microstructural characterisation of high-entropy alloy AlCoCrFeNi fabricated by laser engineered net shaping", *Journal of Alloys and Compounds*, Vol. 648, pp. 751-758.

Ladewig, A., Schlick, G., Fisser, M., Schulze, V. and Glatzel, U. (2016), "Influence of the shielding gas flow on the removal of process by-products in the selective laser melting process", *Additive Manufacturing*, Vol. 10, pp. 1-9.

Lai, C.H., Lin, S.J., Yeh, J.W. and Chang, S.Y. (2006), "Preparation and characterization of AlCrTaTiZr multi-element nitride coatings", *Surface and Coatings Technology*, Vol. 201 No. 6, pp. 3275-3280.

Lal, M.S. and Sundara, R. (2019), "High entropy oxides – a Cost-Effective catalyst for the growth of high yield carbon nanotubes and their energy applications", *ACS Applied Materials & Interfaces*, Vol. 11 No. 34, pp. 30846-30857.

Li, Z. (2019), "Interstitial equiatomic CoCrFeMnNi high-entropy alloys: carbon content, microstructure, and compositional homogeneity effects on deformation behavior", *Acta Materialia*, Vol. 164, pp. 400-412.

Liao, W., Lan, S., Gao, L., Zhang, H., Xu, S., Song, J., Wang, X. and Lu, Y. (2017), "Nanocrystalline high-entropy alloy (CoCrFeNiAl0. 3) thin-film coating by magnetron sputtering", *Thin Solid Films*, Vol. 638, pp. 383-388.

Li, Q., Chen, E.Y., Bice, D.R. and Dunand, D.C. (2008), "Mechanical properties of cast Ti-6Al-4V lattice block structures", *Metallurgical and Materials Transactions A*, Vol. 39 No. 2, pp. 441-449.

Li, J., Craeghs, W., Jing, C., Gong, S. and Shan, F. (2017), "Microstructure and physical performance of laser-induction nanocrystals modified high-entropy alloy composites on titanium alloy", *Materials & Design*, Vol. 117, pp. 363-370.

Li, J., Huang, Y., Meng, X. and Xie, Y. (2019), "A review on high entropy alloys coatings: fabrication processes and property assessment", *Advanced Engineering Materials*, Vol. 21 No. 8, p. 1900343.

Lilensten, L., Couzinié, J., Perrière, L., Bourgon, J., Emery, N. and Guillot, I. (2014), "New structure in refractory high-entropy alloys", *Materials Letters*, Vol. 132, pp. 123-125.

Li, W., Liu, P. and Liaw, P.K. (2018), "Microstructures and properties of high-entropy alloy films and coatings: a review", *Materials Research Letters*, Vol. 6 No. 4, pp. 199-229.

Li, Y. and Nilkitsaranont, P. (2009), "Gas turbine performance prognostic for condition-based maintenance", *Applied Energy*, Vol. 86 No. 10, pp. 2152-2161.

Lin, Y., Nong, F.Q., Chen, X.M., Chen, D.D. and Chen, M.S. (2017), "Microstructural evolution and constitutive models to predict hot deformation behaviors of a nickel-based superalloy", *Vacuum*, Vol. 137, pp. 104-114.

Lin, M.I., Tsai, M.H., Shen, W.J. and Yeh, J.W. (2010), "Evolution of structure and properties of multi-component (AlCrTaTiZr) ox films", *Thin Solid Films*, Vol. 518 No. 10, pp. 2732-2737.

Li, Z. and Raabe, D. (2018), "Influence of compositional inhomogeneity on mechanical behavior of an interstitial dual-phase high-entropy alloy", *Materials Chemistry and Physics*, Vol. 210, pp. 29-36.

Liu, Y., Li, S., Wang, H., Hou, W., Hao, Y., Yang, R., Sercombe, T. and Zhang, L.C. (2016), "Microstructure, defects and mechanical behavior of beta-type titanium porous structures manufactured by electron beam melting and selective laser melting", *Acta Materialia*, Vol. 113, pp. 56-67.

Liu, D., Xiong, Y., Topping, T.D., Zhou, Y., Haines, C., Paras, J., Martin, D., Kapoor, D., Schoenung, J.M. and Lavernia, E.J. (2012), "Spark plasma sintering of cryomilled nanocrystalline Al alloy-Part II: influence of processing conditions on densification and properties", *Metallurgical and Materials Transactions A*, Vol. 43 No. 1, pp. 340-350.

Liu, W., Yang, T. and Liu, C. (2018), "Precipitation hardening in CoCrFeNi-based high entropy alloys", *Materials Chemistry and Physics*, Vol. 210, pp. 2-11.

Li, B., Wang, Y., Ren, M., Yang, C. and Fu, H. (2008), "Effects of Mn, Ti and V on the microstructure and properties of AlCrFeCoNiCu high entropy alloy", *Materials Science and Engineering: A*, Vol. 498 Nos 1/2, pp. 482-486.

Li, N., Wu, S., Ouyang, D., Zhang, J. and Liu, L. (2020), "Fe-based metallic glass reinforced FeCoCrNiMn high entropy alloy through selective laser melting", *Journal of Alloys and Compounds*, Vol. 822 No. 153695.

Li, X., Zheng, Z., Dou, D. and Li, J. (2016), "Microstructure and properties of coating of FeAlCuCrCoMn high entropy alloy deposited by direct current magnetron sputtering", *Materials Research*, Vol. 19 No. 4, pp. 802-806.

Long, Y., Zhang, H., Wang, T., Huang, X., Li, Y., Wu, J. and Chen, H. (2013), "High-strength Ti–6Al–4V with ultrafine-grained structure fabricated by high energy ball milling and spark plasma sintering", *Materials Science and Engineering: A*, Vol. 585, pp. 408-414.

Lu, X., Wang, D., Li, Z., Deng, Y. and Barnoush, A. (2019a), "Hydrogen susceptibility of an interstitial equimolar high-entropy alloy revealed by in-situ electrochemical microcantilever bending test", *Materials Science and Engineering: A*, Vol. 762 No. 138114.

Lu, T.W., Feng, C.S., Wang, Z., Liao, K.W., Liu, Z.Y., Xie, Y.Z., Hu, J.G. and Liao, W.B. (2019b), "Microstructures and mechanical properties of CoCrFeNiAl0. 3 high-entropy alloy thin films by pulsed laser deposition", *Applied Surface Science*, Vol. 494, pp. 72-79.

Lu, X., Liu, T., Zhai, T., Wang, G., Yu, M., Xie, S., Ling, Y., Liang, C., Tong, Y. and LI., Y. (2014), "Improving the cycling stability of metal–nitride supercapacitor electrodes with a thin carbon shell", *Advanced Energy Materials*, Vol. 4 No. 4, p. 1300994.

Madan, P. (2016), "Annealing treatments and high strain rate testing of high entropy alloys".

Makineni, S., Nithin, B. and Chattopadhyay, K. (2015), "Synthesis of a new tungsten-free γ–γ' cobalt-based superalloy by tuning alloying additions", *Acta Materialia*, Vol. 85, pp. 85-94.

Mallick, B.C., Hsieh, C.T., Yin, K.M., Gandomi, Y.A. and Huang, K.T. (2019), "On atomic layer deposition: current progress and future challenges", *ECS Journal of Solid State Science and Technology*, Vol. 8 No. 4, p. N55.

Marazani, T., Madyira, D.M. and Akinlabi, E.T. (2017), "Repair of cracks in metals: a review", *Procedia Manufacturing*, Vol. 8, pp. 673-679.

Marshal, A., Pradeep, K., Music, D., Wang, L., Petracic, O. and Schneider, J. (2019), "Combinatorial evaluation of phase formation and magnetic properties of FeMnCoCrAl high entropy alloy thin film library", *Scientific Reports*, Vol. 9 No. 1, pp. 1-11.

Masanes, L. and Oppenheim, J. (2017), "A general derivation and quantification of the third law of thermodynamics", *Nature Communications*, Vol. 8 No. 1, pp. 1-7.

Mathew, J., Kshirsagar, R., Zabeen, S., Smyth, N., Kanarachos, S., Langer, K. and Fitzpatrick, M.E. (2021), "Machine Learning-Based prediction and optimisation system for laser shock peening", *Applied Sciences*, Vol. 11 No. 7, p. 2888.

Mattox, D.M. (1998), *Handbook of Physical Vapor Deposition (PVD) Processing, Film Formation, Adhesion, Surface Preparation and Contamination Control, 1998*, Dostupné z available at: http://lib.semi.ac.cn,8080

Ma, L., Wang, L., Zhang, T. and Inoue, A. (2002), "Bulk glass formation of Ti-Zr-Hf-Cu-M (M= Fe, Co, Ni) alloys", *Materials Transactions*, Vol. 43 No. 2, pp. 277-280.

Mayrhofer, P.H., Kirnbauer, A., Ertelthaler, P. and Koller, C. M. (2018), "High-entropy ceramic thin films; a case study on transition metal diborides", *Scripta Materialia*, Vol. 149, pp. 93-97.

Ma, S., Zhang, S., Qiao, J., Wang, Z., Gao, M., Jiao, Z., Yang, H. and Zhang, Y. (2014), "Superior high tensile elongation of a single-crystal CoCrFeNiAl0. 3 high-entropy alloy by bridgman solidification", *Intermetallics*, Vol. 54, pp. 104-109.

Meher, S., Aagesen, L., Carroll, M., Pollock, T. and Carroll, L. (2018), "The origin and stability of nanostructural hierarchy in crystalline solids", *Science Advances*, Vol. 4 No. 11, p. eaao6051.

Meisenheimer, P.B., Williams, L.D., Sung, S.H., Gim, J., Shafer, P., Kotsonis, G.N., Maria, J.P., Trassin, M., Hovden, R. and Kioupakis, E. (2019), "Magnetic frustration control through tunable stereochemically driven disorder in entropy-stabilized oxides", *Physical Review Materials*, Vol. 3 No. 10, p. 104420.

Meng, G., Lin, X., Xie, H., Yue, T., Ding, X., Sun, L. and Qi, M. (2016), "The effect of Cu rejection in laser forming of AlCoCrCuFeNi/Mg composite coating", *Materials & Design*, Vol. 108, pp. 157-167.

Meng, G., Yue, T., Lin, X., Yang, H., Xie, H. and Ding, X. (2015), "Laser surface forming of AlCoCrCuFeNi particle reinforced AZ91D matrix composites", *Optics & Laser Technology*, Vol. 70, pp. 119-127.

Mezzapesa, F., Scaraggi, M., Carbone, G., Sorgente, D., Ancona, A. and Lugarà, P. (2013), "Varying the geometry of laser surface microtexturing to enhance the frictional behavior of lubricated steel surfaces", *Physics Procedia*, Vol. 41, pp. 677-682.

Miracle, D.B. (2017), "High-entropy alloys: a current evaluation of founding ideas and core effects and exploring "nonlinear alloys", *JOM*, Vol. 69 No. 11, pp. 2130-2136.

Mirhosseini, N., Crouse, P., Schmidth, M., L.I., L. and Garrod, D. (2007), "Laser surface micro-texturing of Ti–

6Al–4V substrates for improved cell integration", *Applied Surface Science*, Vol. 253 No. 19, pp. 7738-7743.

Mishra, R.K. and Shahi, R.R. (2018), "Magnetic characteristics of high entropy alloys", *Magnetism and Magnetic Materials*, IntechOpen, Rijeka, pp. 67-80.

Mittmann, T., Materano, M., Lomenzo, P.D., Park, M.H., Stolichnov, I., Cavalieri, M., Zhou, C., Chung, C.C., Jones, J.L. and Szyjka, T. (2019), "Origin of ferroelectric phase in undoped HfO2 films deposited by sputtering", *Advanced Materials Interfaces*, Vol. 6 No. 20, p. 1900042.

Mohit, H. and Arul Mozhi Selvan, V. (2018), "A comprehensive review on surface modification, structure interface and bonding mechanism of plant cellulose fiber reinforced polymer based composites", *Composite Interfaces*, Vol. 25 Nos 5/7, pp. 629-667.

Moody, N., Baskes, M., Robinson, S. and Perra, M. (2001), "Temperature effects on hydrogen-induced crack growth susceptibility of iron-based superalloys", *Engineering Fracture Mechanics*, Vol. 68 No. 6, pp. 731-750.

Mozetič, M. (2019), "Surface modification to improve properties of", *Materials*, Vol. 12 No. 3.

Mrdak, M., Medjo, B., Veljić, D., Arsić, M. and Rakin, M. (2019), "The influence of powder feed rate on mechanical properties of atmospheric plasma spray (APS) Al-12Si coating", *Reviews on Advanced Materials Science*, Vol. 58 No. 1, pp. 75-81.

Mugwagwa, L., Dimitrov, D., Matope, S. and Yadroitsev, I. (2018), "Influence of process parameters on residual stress related distortions in selective laser melting".

Nagy, P., Rohbeck, N., Roussely, G., Sortais, P., Lábár, J., Gubicza, J., Michler, J. and Pethö, L. (2020), "Processing and characterization of a multibeam sputtered nanocrystalline CoCrFeNi high-entropy alloy film", *Surface and Coatings Technology*, Vol. 386 No. 125465.

Nahmany, M., Hooper, Z., Stern, A., Geanta, V. and Voiculescu, I. (2016), "Al x CrFeCoNi High-Entropy alloys: surface modification by electron beam bead-on-Plate melting", *Metallography, Microstructure, and Analysis*, Vol. 5 No. 3, pp. 229-240.

Ng, C., Guo, S., Luan, J., Shi, S. and Liu, C.T. (2012), "Entropy-driven phase stability and slow diffusion kinetics in an Al0. 5CoCrCuFeNi high entropy alloy", *Intermetallics*, Vol. 31, pp. 165-172.

Ocelík, V., Janssen, N., Smith, S. and DE Hosson, J.T.M. (2016), "Additive manufacturing of high-entropy alloys by laser processing", *JOM*, Vol. 68 No. 7, pp. 1810-1818.

Ogunbiyi, O., Jamiru, T., Sadiku, E., Adesina, O., Beneke, L. and Adegbola, T. (2019a), "Spark plasma sintering of nickel and nickel based alloys: a review", *Procedia Manufacturing*, Vol. 35, pp. 1324-1329.

Ogunbiyi, O., Sadiku, E., Jamiru, T., Adesina, O. and Beneke, L. (2019b), "Spark plasma sintering of inconel 738LC: densification and microstructural characteristics", *Materials Research Express*, Vol. 6 No. 10, p. 1065g1068.

Olumayegun, O., Wang, M. and Kelsall, G. (2017), "Thermodynamic analysis and preliminary design of closed brayton cycle using nitrogen as working fluid and coupled to small modular sodium-cooled fast reactor (SM-SFR)", *Applied Energy*, Vol. 191, pp. 436-453.

Oses, C., Toher, C. and Curtarolo, S. (2020), "High-entropy ceramics", *Nature Reviews Materials*, Vol. 5 No. 4, pp. 295-309.

Otto, F., Yang, Y., Bei, H. and George, E.P. (2013), "Relative effects of enthalpy and entropy on the phase stability of equiatomic high-entropy alloys", *Acta Materialia*, Vol. 61 No. 7, pp. 2628-2638.

Palanivel, S., Sidhar, H. and Mishra, R. (2015), "Friction stir additive manufacturing: route to high structural performance", *JOM*, Vol. 67 No. 3, pp. 616-621.

Pal, S., Drstvensek, I. and Brajlih, T. (2018), "Physical behaviors of materials in selective laser melting process", *DAAAM Int Sci B*, pp. 239-256.

Pal, S., Tiyyagura, H.R., Drstvenšek, I. and Kumar, C.S. (2016), "The effect of post-processing and machining process parameters on properties of stainless steel PH1 product produced by direct metal laser sintering", *Procedia Engineering*, Vol. 149, pp. 359-365.

Patel, D., Jain, V. and Ramkumar, J. (2018), "Micro texturing on metallic surfaces: state of the art", *Proceedings of the Institution of Mechanical Engineers, Part B: Journal of Engineering Manufacture*, Vol. 232 No. 6, pp. 941-964.

Peters, M., Kumpfert, J., Ward, C.H. and Leyens, C. (2003), "Titanium alloys for aerospace applications", *Advanced Engineering Materials*, Vol. 5 No. 6, pp. 419-427.

Philip, J.T., Mathew, J. and Kuriachen, B. (2019), "Tribology of Ti6Al4V: a review", *Friction*, Vol. 7 No. 6, pp. 497-536.

Phillips, B., Avery, D., LIU., T., Rodriguez, O., Mason, C., Jordon, J., Brewer, L. and Allison, P. (2019), "Microstructure-deformation relationship of additive friction stir-deposition Al–Mg–Si", *Materialia*, Vol. 7 No. 100387.

Pierson, H.O. (1999), *Handbook of Chemical Vapor Deposition: principles, Technology and Applications*, William Andrew.

Piqué, A. and Serra, P. (2018), *Laser Printing of Functional Materials: 3D Microfabrication, Electronics and Biomedicine*, John Wiley & Sons.

Prabu, G., Duraiselvam, M., Jeyaprakash, N. and Yang, C.H. (2020), "Microstructural evolution and wear behavior of AlCoCrCuFeNi high entropy alloy on Ti–6Al–4V through laser surface alloying", *Metals and Materials International*, pp. 1-13.

Pratap, T. and Patra, K. (2018), "Mechanical micro-texturing of Ti-6Al-4V surfaces for improved wettability and bio-tribological performances", *Surface and Coatings Technology*, Vol. 349, pp. 71-81.

Praveen, S., Murty, B. and Kottada, R.S. (2013), "Phase evolution and densification behavior of nanocrystalline multicomponent high entropy alloys during spark plasma sintering", *JOM*, Vol. 65 No. 12, pp. 1797-1804.

Qian, N., Ding, W. and Zhu, Y. (2018), "Comparative investigation on grindability of K4125 and Inconel718 nickel-based superalloys", *The International Journal of Advanced Manufacturing Technology*, Vol. 97 Nos 5/8, pp. 1649-1661.

Qian, M. and Froes, F.H. (2015), "Titanium powder metallurgy: science, technology and applications".

Qin, G., Chen, R., Liaw, P.K., Gao, Y., Wang, L., Su, Y., Ding, H., Guo, J. and Li, X. (2020), "An as-cast high-entropy alloy with remarkable mechanical properties

strengthened by nanometer precipitates", *Nanoscale*, Vol. 12 No. 6, pp. 3965-3976.

Qin, G., Chen, R., Zheng, H., Fang, H., Wang, L., Su, Y., Guo, J. and Fu, H. (2019a), "Strengthening FCC-CoCrFeMnNi high entropy alloys by Mo addition", *Journal of Materials Science & Technology*, Vol. 35 No. 4, pp. 578-583.

Qin, Y., Liu, J.X., L.I., F., Wei, X., Wu, H. and Zhang, G.J. (2019b), "A high entropy silicide by reactive spark plasma sintering", *Journal of Advanced Ceramics*, Vol. 8 No. 1, pp. 148-152.

Qiu, N., Chen, H., Yang, Z., Sun, S., Wang, Y. and Cui, Y. (2019), "A high entropy oxide (Mg0. 2Co0. 2Ni0. 2Cu0. 2Zn0. 2O) with superior lithium storage performance", *Journal of Alloys and Compounds*, Vol. 777, pp. 767-774.

Qiu, Y., Thomas, S., Gibson, M.A., Fraser, H.L. and Birbilis, N. (2017), *Npj Materials Degradation*, Vol. 1 No. 1, pp. 1-18.

Raabe, D., Tasan, C.C., Springer, H. and Bausch, M. (2015), "From high-entropy alloys to high-entropy steels", *Steel Research International*, Vol. 86 No. 10, pp. 1127-1138.

Ramappa, D.A. and Jogikalmath, G. (2018), "Methods for surface modification of materials. Google patents".

Redka, D., Gadelmeier, C., Winter, J., Spellauge, M., Eulenkamp, C., Calta, P., Glatzel, U., Minár, J. and Huber, H.P. (2021), "Sub-picosecond single-pulse laser ablation of the CrMnFeCoNi high entropy alloy and comparison to stainless steel AISI 304", *Applied Surface Science*, Vol. 544, p. 148839.

Rogal, Ł., Kalita, D., Tarasek, A., Bobrowski, P. and Czerwinski, F. (2017), "Effect of SiC nano-particles on microstructure and mechanical properties of the CoCrFeMnNi high entropy alloy", *Journal of Alloys and Compounds*, Vol. 708, pp. 344-352.

Rost, C., Sachet, E., Borman, T., Mionsoballegh, A., Dickey, E., Hou, D., Jones, J., Curtarolo, S. and Maria, J. (2015a), "Entropy-stabilized oxides", *Nature Communications*, Vol. 6 No. 1, p. 8485.

Rost, C.M., Sachet, E., Borman, T., Moballegh, A., Dickey, E. C., Hou, D., Jones, J.L., Curtarolo, S. and Maria, J.P. (2015b), "Entropy-stabilized oxides", *Nature Communications*, Vol. 6 No. 1, pp. 1-8.

Rötting, O., Röpke, W., Becker, H. and Gärtner, C. (2002), "Polymer microfabrication technologies", *Microsystem Technologies*, Vol. 8 No. 1, pp. 32-36.

Rubenchik, A., Feit, M., Perry, M. and Larsen, J. (1998), "Numerical simulation of ultra-short laser pulse energy deposition and bulk transport for material processing", *Applied Surface Science*, Vol. 127, pp. 193-198.

Rusanov, A.I. (2016), "Thermodynamic aspects of materials science", *Russian Chemical Reviews*, Vol. 85 No. 1, p. 1.

Russo, R.E., Mao, X., Liu, H., Gonzalez, J. and Mao, S.S. (2002), "Laser ablation in analytical chemistry – a review", *Talanta*, Vol. 57 No. 3, pp. 425-451.

Saeed-Akbari, A., Imlau, J., Prahl, U. and Bleck, W. (2009), "Derivation and variation in composition-dependent stacking fault energy maps based on subregular solution model in high-manganese steels", *Metallurgical and Materials Transactions A*, Vol. 40 No. 13, pp. 3076-3090.

Saito, T., Ishida, A., Yuyama, M., Takata, Y., Kawagishi, K., Yeh, A.C. and Murakami, H. (2021), "Tensile creep behavior of Single-Crystal High-Entropy superalloy at intermediate temperature", *Crystals*, Vol. 11 No. 1, p. 28.

Salishchev, G., Tikhonovsky, M., Shaysultanov, D., Stepanov, N., Kuznetsov, A., Kolodiy, I., Tortika, A. and Senkov, O. (2014), "Effect of Mn and V on structure and mechanical properties of high-entropy alloys based on CoCrFeNi system", *Journal of Alloys and Compounds*, Vol. 591, pp. 11-21.

Santo, L. (2008), "Laser cladding of metals: a review", *International Journal of Surface Science and Engineering*, Vol. 2 No. 5, pp. 327-336.

Sarkar, A., Djenadic, R., Usharani, N.J., Sanghvi, K.P., Chakravadhanula, V.S., Gandhi, A.S., Hahn, H. and Bhattacharya, S.S. (2017a), "Nanocrystalline multicomponent entropy stabilised transition metal oxides", *Journal of the European Ceramic Society*, Vol. 37 No. 2, pp. 747-754.

Sarkar, A., Loho, C., Velasco, L., Thomas, T., Bhattacharya, S.S., Hahn, H. and Djenadic, R. (2017b), "Multicomponent equiatomic rare earth oxides with a narrow band gap and associated praseodymium multivalency", *Dalton Transactions*, Vol. 46 No. 36, pp. 12167-12176.

Schroers, J. (2010), "Processing of bulk metallic glass", *Advanced Materials*, Vol. 22 No. 14, pp. 1566-1597.

Seifi, M., Gorelik, M., Waller, J., Hrabe, N., Shamsaei, N., Daniewicz, S. and Lewandowski, J.J. (2017), "Progress towards metal additive manufacturing standardization to support qualification and certification", *JOM*, Vol. 69 No. 3, pp. 439-455.

Sekkat, Z. and Kawata, S. (2014), "Laser nanofabrication in photoresists and azopolymers", *Laser & Photonics Reviews*, Vol. 8 No. 1, pp. 1-26.

Senkov, O.N., Isheim, D., Seidman, D.N. and Pilchak, A.L. (2016), "Development of a refractory high entropy superalloy", *Entropy*, Vol. 18 No. 3, p. 102.

Senkov, O., Jensen, J., Pilchak, A., Miracle, D. and Fraser, H. (2018a), "Compositional variation effects on the microstructure and properties of a refractory high-entropy superalloy AlMo0. 5NbTa0. 5TiZr", *Materials & Design*, Vol. 139, pp. 498-511.

Senkov, O.N., Miracle, D.B., Chaput, K.J. and Couzinie, J.P. (2018b), "Development and exploration of refractory high entropy alloys – a review", *Journal of Materials Research*, Vol. 33 No. 19, pp. 3092-3128.

Senkov, O., Senkova, S. and Woodward, C. (2014), "Effect of aluminum on the microstructure and properties of two refractory high-entropy alloys", *Acta Materialia*, Vol. 68, pp. 214-228.

Senkov, O., Wilks, G., Miracle, D., Chuang, C. and Liaw, P. (2010), "Refractory high-entropy alloys", *Intermetallics*, Vol. 18 No. 9, pp. 1758-1765.

Seol, J.B., Bae, J.W., Kim, J.G., Sung, H., L.I., Z., Lee, H.H., Shim, S.H., Jang, J.H., Ko, W.S. and Hong, S.I. (2020), "Short-range order strengthening in boron-doped high-entropy alloys for cryogenic applications", *Acta Materialia*, Vol. 194, pp. 366-377.

Sharma, Y., Musico, B.L., Gao, X., Hua, C., May, A.F., Herklotz, A., Rastogi, A., Mandrus, D., Yan, J. and Lee, H.N. (2018), "Single-crystal high entropy perovskite oxide

epitaxial films", *Physical Review Materials*, Vol. 2 No. 6, p. 060404.

Shinde, M.S. and Ashtankar, K.M. (2017), "Additive manufacturing–assisted conformal cooling channels in mold manufacturing processes", *Advances in Mechanical Engineering*, Vol. 9 No. 5, p. 1687814017699764.

Shukla, S., Wang, T., Frank, M., Agrawal, P., Sinha, S., Mirshams, R. and Mishra, R.S. (2020), "Friction stir gradient alloying: a novel solid-state high throughput screening technique for high entropy alloys", *Materials Today Communications*, Vol. 23 No. 100869.

Shu, F., Wu, L., Zhao, H., Sui, S., Zhou, L., Zhang, J., He, W., He, P. and Xu, B. (2018a), "Microstructure and high-temperature wear mechanism of laser cladded CoCrBFeNiSi high-entropy alloy amorphous coating", *Materials Letters*, Vol. 211, pp. 235-238.

Shu, F., Yang, B., Dong, S., Zhao, H., Xu, B., Xu, F., Liu, B., He, P. and Feng, J. (2018b), "Effects of Fe-to-Co ratio on microstructure and mechanical properties of laser cladded FeCoCrBNiSi high-entropy alloy coatings", *Applied Surface Science*, Vol. 450, pp. 538-544.

Sidhu, T., Malik, A., Prakash, S. and Agrawal, R. (2007), "Oxidation and hot corrosion resistance of HVOF WC-NiCrFeSiB coating on Ni-and Fe-based superalloys at 800 C", *Journal of Thermal Spray Technology*, Vol. 16 Nos 5/6, pp. 844-849.

Sohrabi, N., Jhabvala, J., Kurtuldu, G., Stoica, M., Parrilli, A., Berns, S., Polatidis, E., VAN Petegem, S., Hugon, S. and Neels, A. (2021), "Characterization, mechanical properties and dimensional accuracy of a Zr-based bulk metallic glass manufactured via laser powder-bed fusion", *Materials & Design*, Vol. 199 No. 109400.

Song, W., Radulescu, A., Liu, L. and Bleck, W. (2017), "Study on a high entropy alloy by high energy synchrotron X-ray diffraction and small angle neutron scattering", *Steel Research International*, Vol. 88 No. 10, p. 1700079.

Soni, V., Senkov, O., Gwalani, B., Miracle, D. and Banerjee, R. (2018), "Microstructural design for improving ductility of an initially brittle refractory high entropy alloy", *Scientific Reports*, Vol. 8 No. 1, pp. 1-10.

Starr, T.L., Rafi, K., Stucker, B. and Scherzer, C.M. (2012), "Controlling phase composition in selective laser melted stainless steels", *Power (W)*, Vol. 195 No. 195, p. 1.

Sun, H.B., Maeda, M., Takada, K., Chon, J.W., Gu, M. and Kawata, S. (2003), "Experimental investigation of single voxels for laser nanofabrication via two-photon photopolymerization", *Applied Physics Letters*, Vol. 83 No. 5, pp. 819-821.

Szemkus, S., Kempf, B., Jahn, S., Wiehl, G., Heringhaus, F. and Rettenmayr, M. (2018), "Laser additive manufacturing of contact materials", *Journal of Materials Processing Technology*, Vol. 252, pp. 612-617.

Tabachnikova, E., Laktionova, M., Semerenko, Y.A., Shumilin, S., Podolskiy, A., Tikhonovsky, M., Miskuf, J., Jurikova, A. and Csach, K. (2017), "Mechanical properties of Al0. 5CoCrCuFeNi high entropy alloy in different structural states in temperature range 0.5–300 K", *Low. Temp. Phys*, Vol. 43, p. N9.

Tan, L., Ren, X., Sridharan, K. and Allen, T. (2008), "Effect of shot-peening on the oxidation of alloy 800H exposed to supercritical water and cyclic oxidation", *Corrosion Science*, Vol. 50 No. 7, pp. 2040-2046.

Tancret, F., Toda-Caraballo, I., Menou, E. and Díaz-DEL, P. E.J.R. (2017), "Designing high entropy alloys employing thermodynamics and gaussian process statistical analysis", *Materials & Design*, Vol. 115, pp. 486-497.

Tang, M. and Pistorius, P.C. (2017), "Oxides, porosity and fatigue performance of AlSi10Mg parts produced by selective laser melting", *International Journal of Fatigue*, Vol. 94, pp. 192-201.

Tang, W.Y. and Yeh, J.W. (2009), "Effect of aluminum content on plasma-nitrided Al x CoCrCuFeNi high-entropy alloys", *Metallurgical and Materials Transactions A*, Vol. 40 No. 6, pp. 1479-1486.

Tang, Z., Yuan, T., Tsai, C.W., Yeh, J.W., Lundin, C.D. and Liaw, P.K. (2015a), "Fatigue behavior of a wrought Al0. 5CoCrCuFeNi two-phase high-entropy alloy", *Acta Materialia*, Vol. 99, pp. 247-258.

Tang, Z., Yuan, T., Tsai, C.W., Yeh, J.W., Lundin, C.D. and Liaw, P.K. (2015b), "Fatigue behavior of a wrought Al 0.5 CoCrCuFeNi two-phase high-entropy alloy", *Acta Materialia*, Vol. 99, pp. 247-258.

Thampy, V., Fong, A.Y., Calta, N.P., Wang, J., Martin, A.A., Depond, P.J., Kiss, A.M., Guss, G., Xing, Q. and Ott, R.T. (2020), "Subsurface cooling rates and microstructural response during laser based metal additive manufacturing", *Scientific Reports*, Vol. 10 No. 1, pp. 1-9.

Thijs, L., Verhaeghe, F., Craeghs, T., VAN Humbeeck, J. and Kruth, J.P. (2010), "A study of the microstructural evolution during selective laser melting of Ti–6Al–4V", *Acta Materialia*, Vol. 58 No. 9, pp. 3303-3312.

Tian, Y., Chen, C., L.I., S. and Huo, Q. (2005), "Research progress on laser surface modification of titanium alloys", *Applied Surface Science*, Vol. 242 Nos 1/2, pp. 177-184.

Tian, X., Zhao, J., Qin, W., Gong, F., Wang, Y. and Pan, H. (2017), "Performance of ceramic tools in high-speed cutting iron-based superalloys", *Machining Science and Technology*, Vol. 21 No. 2, pp. 279-290.

Tirado, F.L.R., Taylor, S. and Dunand, D.C. (2019), "Effect of Al, Ti and Cr additions on the γ-γ'microstructure of W-free Co-Ta-V-Based superalloys", *Acta Materialia*, Vol. 172, pp. 44-54.

Tong, C.J., Chen, M.R., Yeh, J.W., Lin, S.J., Chen, S.K., Shun, T.T. and Chang, S.Y. (2005), "Mechanical performance of the Al x CoCrCuFeNi high-entropy alloy system with multiprincipal elements", *Metallurgical and Materials Transactions A*, Vol. 36 No. 5, pp. 1263-1271.

Tong, Z., Ren, X., Jiao, J., Zhou, W., Ren, Y., Ye, Y., Larson, E.A. and Gu, J. (2019), "Laser additive manufacturing of FeCrCoMnNi high-entropy alloy: effect of heat treatment on microstructure, residual stress and mechanical property", *Journal of Alloys and Compounds*, Vol. 785, pp. 1144-1159.

Trexler, M.M. and Thadhani, N.N. (2010), "Mechanical properties of bulk metallic glasses", *Progress in Materials Science*, Vol. 55 No. 8, pp. 759-839.

Tsai, C.W., Chen, Y.L., Tsai, M.H., Yeh, J.W., Shun, T.T. and Chen, S.K. (2009), "Deformation and annealing behaviors of high-entropy alloy Al0. 5CoCrCuFeNi", *Journal of Alloys and Compounds*, Vol. 486 Nos 1/2, pp. 427-435.

Tsao, T.K., Yeh, A.C. and Murakami, H. (2017), "The microstructure stability of precipitation strengthened medium to high entropy superalloys", *Metallurgical and Materials Transactions A*, Vol. 48 No. 5, pp. 2435-2442.

Uchida, M., Nihira, N., Mitsuo, A., Toyoda, K., Kubota, K. and Aizawa, T. (2004), "Friction and wear properties of CrAlN and CrVN films deposited by cathodic arc ion plating method", *Surface and Coatings Technology*, Vol. 177, pp. 627-630.

Varalakshmi, S., Kamaraj, M. and Murty, B. (2008), "Synthesis and characterization of nanocrystalline AlFeTiCrZnCu high entropy solid solution by mechanical alloying", *Journal of Alloys and Compounds*, Vol. 460 Nos 1/2, pp. 253-257.

Varalakshmi, S., Kamaraj, M. and Murty, B. (2010), "Processing and properties of nanocrystalline CuNiCoZnAlTi high entropy alloys by mechanical alloying", *Materials Science and Engineering: A*, Vol. 527 Nos 4/5, pp. 1027-1030.

Vilaro, T., Colin, C. and Bartout, J.D. (2011), "As-fabricated and heat-treated microstructures of the Ti-6Al-4V alloy processed by selective laser melting", *Metallurgical and Materials Transactions A*, Vol. 42 No. 10, pp. 3190-3199.

Vilaro, T., Colin, C., Bartout, J.D., Nazé, L. and Sennour, M. (2012), "Microstructural and mechanical approaches of the selective laser melting process applied to a nickel-base superalloy", *Materials Science and Engineering: A*, Vol. 534, pp. 446-451.

Vilhena, L., Sedlaček, M., Podgornik, B., Vižintin, J., Babnik, A. and Možina, J. (2009), "Surface texturing by pulsed Nd: YAG laser", *Tribology International*, Vol. 42 No. 10, pp. 1496-1504.

Viteri, F. and Anderson, R.E. (2003), *Semi-Closed Brayton Cycle Gas Turbine Power Systems*, Google Patents.

Voldman, J., Gray, M.L. and Schmidt, M.A. (1999), "Microfabrication in biology and medicine", *Annual Review of Biomedical Engineering*, Vol. 1 No. 1, pp. 401-425.

Walsh, P.P. and Fletcher, P. (2005), *Gas Turbine Engine*, Google Patents.

Wang, X., Carter, L.N., Pang, B., Attallah, M.M. and Loretto, M.H. (2017), "Microstructure and yield strength of SLM-fabricated CM247LC Ni-Superalloy", *Acta Materialia*, Vol. 128, pp. 87-95.

Wang, W.H., Dong, C. and Shek, C. (2004), "Bulk metallic glasses", *Materials Science and Engineering: R: Reports*, Vol. 44 Nos 2/3, pp. 45-89.

Wang, Y.P., Li, B.S. and Fu, H.Z. (2009), "Solid solution or intermetallics in a high-entropy alloy", *Advanced Engineering Materials*, Vol. 11 No. 8, pp. 641-644.

Wang, F., Li, Y., Ziefuß, A.R., Bertin, E., Kamp, M., Duppel, V., Marzun, G., Kienle, L., Barcikowski, S. and Gökce, B. (2019a), "Kinetically-controlled laser-synthesis of colloidal high-entropy alloy nanoparticles", *RSC Advances*, Vol. 9 No. 32, pp. 18547-18558.

Wang, X., Huang, Z., Cai, B., Zhou, N., Magdysyuk, O., Gao, Y., Srivatsa, S., Tan, L. and Jiang, L. (2019b), "Formation mechanism of abnormally large grains in a polycrystalline nickel-based superalloy during heat treatment processing", *Acta Materialia*, Vol. 168, pp. 287-298.

Wang, C., Li, T.H., Liao, Y.C., Li, C.L., Jang, J.S.C. and Hsueh, C.H. (2019c), "Hardness and strength enhancements of CoCrFeMnNi high-entropy alloy with Nd doping", *Materials Science and Engineering: A*, Vol. 764 No. 138192.

Wang, T., Shukla, S., Komarasamy, M., Liu, K. and Mishra, R.S. (2019d), "Towards heterogeneous AlxCoCrFeNi high entropy alloy via friction stir processing", *Materials Letters*, Vol. 236, pp. 472-475.

Wang, Q., Sarkar, A., L.I., Z., Lu, Y., Velasco, L., Bhattacharya, S.S., Brezesinski, T., Hahn, H. and Breitung, B. (2019e), "High entropy oxides as anode material for Li-ion battery applications: a practical approach", *Electrochemistry Communications*, Vol. 100, pp. 121-125.

Wang, C., Li, X., L.I., Z., Wang, Q., Zheng, Y., Ma, Y., Bi, L., Zhang, Y., Yuan, X. and Zhang, X. (2020a), "The resistivity–temperature behavior of AlxCoCrFeNi high-entropy alloy films", *Thin Solid Films*, Vol. 700 No. 137895.

Wang, Z., Wang, C., Zhao, Y.L., Hsu, Y.C., Li, C.L., Kai, J.J., Liu, C.T. and Hsueh, C.H. (2020b), "High hardness and fatigue resistance of CoCrFeMnNi high entropy alloy films with ultrahigh-density nanotwins", *International Journal of Plasticity*, Vol. 131 No. 102726.

Wang, Z., Wang, C., Zhao, Y.L., Huang, T.H., Li, C.L., Kai, J.J., Liu, C.T. and Hsueh, C.H. (2020c), "Growth, microstructure and mechanical properties of CoCrFeMnNi high entropy alloy films", *Vacuum*, Vol. 179 No. 109553.

Wang, R., Zhang, K., Davies, C. and Wu, X. (2017), "Evolution of microstructure, mechanical and corrosion properties of AlCoCrFeNi high-entropy alloy prepared by direct laser fabrication", *Journal of Alloys and Compounds*, Vol. 694, pp. 971-981.

Wen, T., L.I.U., H., Ye, B., Liu, D. and Chu, Y. (2020), "High-entropy alumino-silicides: a novel class of high-entropy ceramics", *Science China Materials*, Vol. 63 No. 2, pp. 300-306.

Whitfield, T., Pickering, E., Owen, L., Jones, C., Stone, H. and Jones, N. (2020), "The effect of Al on the formation and stability of a BCC–B2 microstructure in a refractory metal high entropy superalloy system", *Materialia*, Vol. 13 No. 100858.

Whitfield, T.E., Pickering, E.J., Owen, L.R., Senkov, O.N., Miracle, D.B., Stone, H.J. and Jones, N.G. (2021a), "An assessment of the thermal stability of refractory high entropy superalloys", *Journal of Alloys and Compounds*, Vol. 857 No. 157583.

Whitfield, T.E., Stone, H.J., Jones, C.N. and Jones, N.G. (2021b), "Microstructural degradation of the AlMo0. 5NbTa0. 5TiZr refractory metal High-Entropy superalloy at elevated temperatures", *Entropy*, Vol. 23 No. 1, p. 80.

Willmott, P. and Huber, J. (2000), "Pulsed laser vaporization and deposition", *Reviews of Modern Physics*, Vol. 72 No. 1, p. 315.

Wong, K.V. and Hernandez, A. (2012), "A review of additive manufacturing", *International Scholarly Research Notices*, Vol. 2012.

Wright, A.J. and Luo, J. (2020), "A step forward from high-entropy ceramics to compositionally complex ceramics: a new perspective", *Journal of Materials Science*, Vol. 55 No. 23, pp. 9812-9827.

Wright, A.J., Wang, Q., Huang, C., Nieto, A., Chen, R. and Luo, J. (2020), "From high-entropy ceramics to

compositionally-complex ceramics: a case study of fluorite oxides", *Journal of the European Ceramic Society*, Vol. 40 No. 5, pp. 2120-2129.

Wu, J.M., Lin, S.J., Yeh, J.W., Chen, S.K., Huang, Y.S. and Chen, H.C. (2006), "Adhesive wear behavior of AlxCoCrCuFeNi high-entropy alloys as a function of aluminum content", *Wear*, Vol. 261 Nos 5/6, pp. 513-519.

Wu, Z., Parish, C. and Bei, H. (2015), "Nano-twin mediated plasticity in carbon-containing FeNiCoCrMn high entropy alloys", *Journal of Alloys and Compounds*, Vol. 647, pp. 815-822.

Wu, C., Zhang, S., Zhang, C., Zhang, H. and Dong, S. (2017), "Phase evolution and cavitation erosion-corrosion behavior of FeCoCrAlNiTix high entropy alloy coatings on 304 stainless steel by laser surface alloying", *Journal of Alloys and Compounds*, Vol. 698, pp. 761-770.

Xiao, R., Hong, M., Liu, J., Yao, J. and Sano, Y. (2018), "Advanced laser processing and manufacturing III", *Advanced Laser Processing and Manufacturing II*, p. 10813.

Xiaotao, L., Wenbin, L., Lijuan, M., Jinling, L., Jing, L. and Jianzhong, C. (2016), "Effect of boron on the microstructure, phase assemblage and wear properties of Al0. 5CoCrCuFeNi High-Entropy alloy", *Rare Metal Materials and Engineering*, Vol. 45 No. 9, pp. 2201-2207.

Xing, Q., Wang, H., Chen, M., Chen, Z., Li, R., Jin, P. and Zhang, Y. (2019), "Mechanical properties and corrosion resistance of NbTiAlSiZrNx high-entropy films prepared by RF magnetron sputtering", *Entropy*, Vol. 21 No. 4, p. 396.

Xu, H., Lu, Y., Liu, Z. and Wang, G. (2019), "Laser 3D printing of Zr-based bulk metallic glass", *Journal of Manufacturing Processes*, Vol. 39, pp. 102-105.

Yan, L., Chen, X., L.I., W., Newkirk, J. and Liou, F. (2016), "Direct laser deposition of Ti-6Al-4V from elemental powder blends", *Rapid Prototyping Journal*, Vol. 22 No. 5.

Yang, C.C., Chau, J.L.H., Weng, C.J., Chen, C.S. and Chou, Y. H. (2017), "Preparation of high-entropy AlCoCrCuFeNiSi alloy powders by gas atomization process", *Materials Chemistry and Physics*, Vol. 202, pp. 151-158.

Yang, X., Dong, P., Yan, Z., Cheng, B., Zhai, X., Chen, H., Zhang, H. and Wang, W. (2020), "AlCoCrFeNi high-entropy alloy particle reinforced 5083Al matrix composites with fine grain structure fabricated by submerged friction stir processing", *Journal of Alloys and Compounds*, Vol. 836 No. 155411.

Yang, T., Zhao, Y., Tong, Y., Jiao, Z., Wei, J., Cai, J., Han, X., Chen, D., Hu, A. and Kai, J. (2018), "Multicomponent intermetallic nanoparticles and superb mechanical behaviors of complex alloys", *Science*, Vol. 362 No. 6417, pp. 933-937.

Yan, M. and Yu, P. (2015), "An overview of densification, microstructure and mechanical property of additively manufactured Ti-6Al-4V – comparison among selective laser melting, electron beam melting, laser metal deposition and selective laser sintering, and with conventional powder", *Sintering Techniques of Materials*.

Yan, X., Zheng, J., Zheng, L., Lin, G., Lin, H., Chen, G., Du, B. and Zhang, F. (2018a), "Optimization of sputtering NiOx films for perovskite solar cell applications", *Materials Research Bulletin*, Vol. 103, pp. 150-157.

Yan, X.H., Li, J.S., Zhang, W.R. and Zhang, Y. (2018b), "A brief review of high-entropy films", *Materials Chemistry and Physics*, Vol. 210, pp. 12-19.

Yao, Y., Huang, Z., Xie, P., Lacey, S.D., Jacob, R.J., Xie, H., Chen, F., Nie, A., Pu, T. and Rehwoldt, M. (2018), "Carbothermal shock synthesis of high-entropy-alloy nanoparticles", *Science*, Vol. 359 No. 6383, pp. 1489-1494.

Yeh, J.W. (2013), "Alloy design strategies and future trends in high-entropy alloys", *JOM*, Vol. 65 No. 12, pp. 1759-1771.

Yeh, J.W., Chen, S.K., Lin, S.J., Gan, J.Y., Chin, T.S., Shun, T.T., Tsau, C.H. and Chang, S.Y. (2004), "Nanostructured high-entropy alloys with multiple principal elements: novel alloy design concepts and outcomes", *Advanced Engineering Materials*, Vol. 6 No. 5, pp. 299-303.

Yeh, J.W. and Lin, S.J. (2018), "Breakthrough applications of high-entropy materials", *Journal of Materials Research*, Vol. 33 No. 19, pp. 3129-3137.

Yeh, A.C. and Tsao, T.K. (2019), *High-Entropy Superalloy*, Google Patents.

Ye, Y., Ouyang, B., Liu, C., Duscher, G. and Nieh, T. (2020), "Effect of interstitial oxygen and nitrogen on incipient plasticity of NbTiZrHf high-entropy alloys", *Acta Materialia*, Vol. 199, pp. 413-424.

Ye, Y., Wang, Q., Lu, J., Liu, C. and Yang, Y. (2016), "High-entropy alloy: challenges and prospects", *Materials Today*, Vol. 19 No. 6, pp. 349-362.

Ye, B., Wen, T., Nguyen, M.C., Hao, L., Wang, C.Z. and Chu, Y. (2019), "First-principles study, fabrication and characterization of (Zr0. 25Nb0. 25Ti0. 25V0. 25) C high-entropy ceramics", *Acta Materialia*, Vol. 170, pp. 15-23.

Yue, T., Xie, H., Lin, X., Yang, H. and Meng, G. (2014), "Solidification behaviour in laser cladding of AlCoCrCuFeNi high-entropy alloy on magnesium substrates", *Journal of Alloys and Compounds*, Vol. 587, pp. 588-593.

Yue, T.M., Xie, H., Lin, X., Yang, H. and Meng, G. (2013), "Microstructure of laser re-melted AlCoCrCuFeNi high entropy alloy coatings produced by plasma spraying", *Entropy*, Vol. 15 No. 12, pp. 2833-2845.

Zalden, P., Quirin, F., Schumacher, M., Siegel, J., Wei, S., Koc, A., Nicoul, M., Trigo, M., Andreasson, P. and Enquist, H. (2019), "Femtosecond x-ray diffraction reveals a liquid–liquid phase transition in phase-change materials", *Science*, Vol. 364 No. 6445, pp. 1062-1067.

Zhai, S., Rojas, J., Ahlborg, N., Lim, K., Toney, M.F., Jin, H., Chueh, W.C. and Majumdar, A. (2018), "The use of poly-cation oxides to lower the temperature of two-step thermochemical water splitting", *Energy & Environmental Science*, Vol. 11 No. 8, pp. 2172-2178.

Zhang, Y. (2019), *High-Entropy Materials*, Springer.

Zhang, T., Fujisawa, K., Zhang, F., LIU., M., Lucking, M.C., Gontijo, R.N., Lei, Y., LIU., H., Crust, K. and Granzier-Nakajima, T. (2020), "Universal in situ substitutional doping of transition metal dichalcogenides by liquid-phase precursor-assisted synthesis", *ACS Nano*, Vol. 14 No. 4, pp. 4326-4335.

Zhang, L., Zhou, Y., Jin, X., Du, X. and LI., B. (2018a), "The microstructure and high-temperature properties of novel nano precipitation-hardened face centered cubic high-entropy superalloys", *Scripta Materialia*, Vol. 146, pp. 226-230.

Zhang, R.Z., Gucci, F., Zhu, H., Chen, K. and Reece, M.J. (2018b), "Data-driven design of ecofriendly thermoelectric

high-entropy sulfides", *Inorganic Chemistry*, Vol. 57 No. 20, pp. 13027-13033.
Zhang, X., Liu, R., Chen, K. and Yao, M. (2013), "Investigation of corrosion behavior of wrought Co-Cr-W super alloys", *CORROSION*, Vol. 2013, OnePetro.
Zhang, Y., Yang, X. and Liaw, P. (2012a), "Alloy design and properties optimization of high-entropy alloys", *JOM*, Vol. 64 No. 7, pp. 830-838.
Zhang, Y., Ma, S. and Qiao, J. (2012b), "Morphology transition from dendrites to equiaxed grains for AlCoCrFeNi high-entropy alloys by copper mold casting and bridgman solidification", *Metallurgical and Materials Transactions A*, Vol. 43 No. 8, pp. 2625-2630.
Zhang, D., Men, L. and Chen, Q. (2011), "Microfabrication and applications of opto-microfluidic sensors", *Sensors*, Vol. 11 No. 5, pp. 5360-5382.
Zhang, R.Z. and Reece, M. J. (2019), "Review of high entropy ceramics: design, synthesis, structure and properties", *Journal of Materials Chemistry A*, Vol. 7 No. 39, pp. 22148-22162.
Zhang, S., Wu, C., Y.I., J. and Zhang, C. (2015), "Synthesis and characterization of FeCoCrAlCu high-entropy alloy coating by laser surface alloying", *Surface and Coatings Technology*, Vol. 262, pp. 64-69.
Zhang, X., Zhang, Y., Lu, J., Xuan, F., Wang, Z. and Tu, S. (2010), "Improvement of fatigue life of Ti–6Al–4V alloy by laser shock peening", *Materials Science and Engineering: A*, Vol. 527 No. 15, pp. 3411-3415.
Zhang, Y., Zhang, L. and Zhou, C. (2013), "Review of chemical vapor deposition of graphene and related applications", *Accounts of Chemical Research*, Vol. 46 No. 10, pp. 2329-2339.
Zhang, Y. and Zhou, Y.J. (2007), "Solid solution formation criteria for high entropy alloys", *Materials Science Forum*, Vols 561/565, pp. 1337-1339.
Zhao, K., Xia, X., Bai, H., Zhao, D. and Wang, W. (2011), "Room temperature homogeneous flow in a bulk metallic glass with low glass transition temperature", *Applied Physics Letters*, Vol. 98 No. 14, p. 141913.
Zheng, B., Zhou, Y., Smugeresky, J., Schoenung, J. and Lavernia, E. (2008a), "Thermal behavior and microstructural evolution during laser deposition with laser-engineered net shaping: part I", *Metallurgical and Materials Transactions A*, Vol. 39 No. 9, pp. 2228-2236.
Zheng, B., Zhou, Y., Smugeresky, J., Schoenung, J. and Lavernia, E. (2008b), "Thermal behavior and microstructure evolution during laser deposition with laser-engineered net shaping: part II", *Metallurgical and Materials Transactions A*, Vol. 39 No. 9, pp. 2237-2245.
Zhu, G., Li, D., Zhang, A., Pi, G. and Tang, Y. (2012), "The influence of laser and powder defocusing characteristics on the surface quality in laser direct metal deposition", *Optics & Laser Technology*, Vol. 44 No. 2, pp. 349-356.
Zhu, Z., Nguyen, Q., Ng, F., An, X., Liao, X., Liaw, P., Nai, S. and Wei, J. (2018), "Hierarchical microstructure and strengthening mechanisms of a CoCrFeNiMn high entropy alloy additively manufactured by selective laser melting", *Scripta Materialia*, Vol. 154, pp. 20-24.
Zou, Y., Wheeler, J.M., Ma, H., Okle, P. and Spolenak, R. (2017), "Nanocrystalline high-entropy alloys: a new paradigm in high-temperature strength and stability", *Nano Letters*, Vol. 17 No. 3, pp. 1569-1574.
Zou, Y., Wu, Y., Li, K., Tan, C., Qiu, Z. and Zeng, D. (2020), "Selective laser melting of crack-free Fe-based bulk metallic glass via chessboard scanning strategy", *Materials Letters*, Vol. 272 No. 127824.

Corresponding author

Modupeola Dada can be contacted at: dadadupeola@gmail.com